© 2018. Published by The Company of Biologists Ltd | Development (2018) 145, dev165910. doi:10.1242/dev.165910

CORRECTION

Correction: Fat body glycogen serves as a metabolic safeguard for the maintenance of sugar levels in *Drosophila* (doi:10.1242/dev.158865)

Takayuki Yamada, Okiko Habara, Hitomi Kubo and Takashi Nishimura

There was an error published in *Development* (2018) **145**, dev158865 (doi:10.1242/dev.158865).

In Fig. 1A, the CNS control panel (top) incorrectly showed a duplicate of the GlyP-RNAi panel (bottom). The corrected Fig. 1 appears below.

This error does not affect the conclusions of the paper. The authors apologise to readers for this mistake.

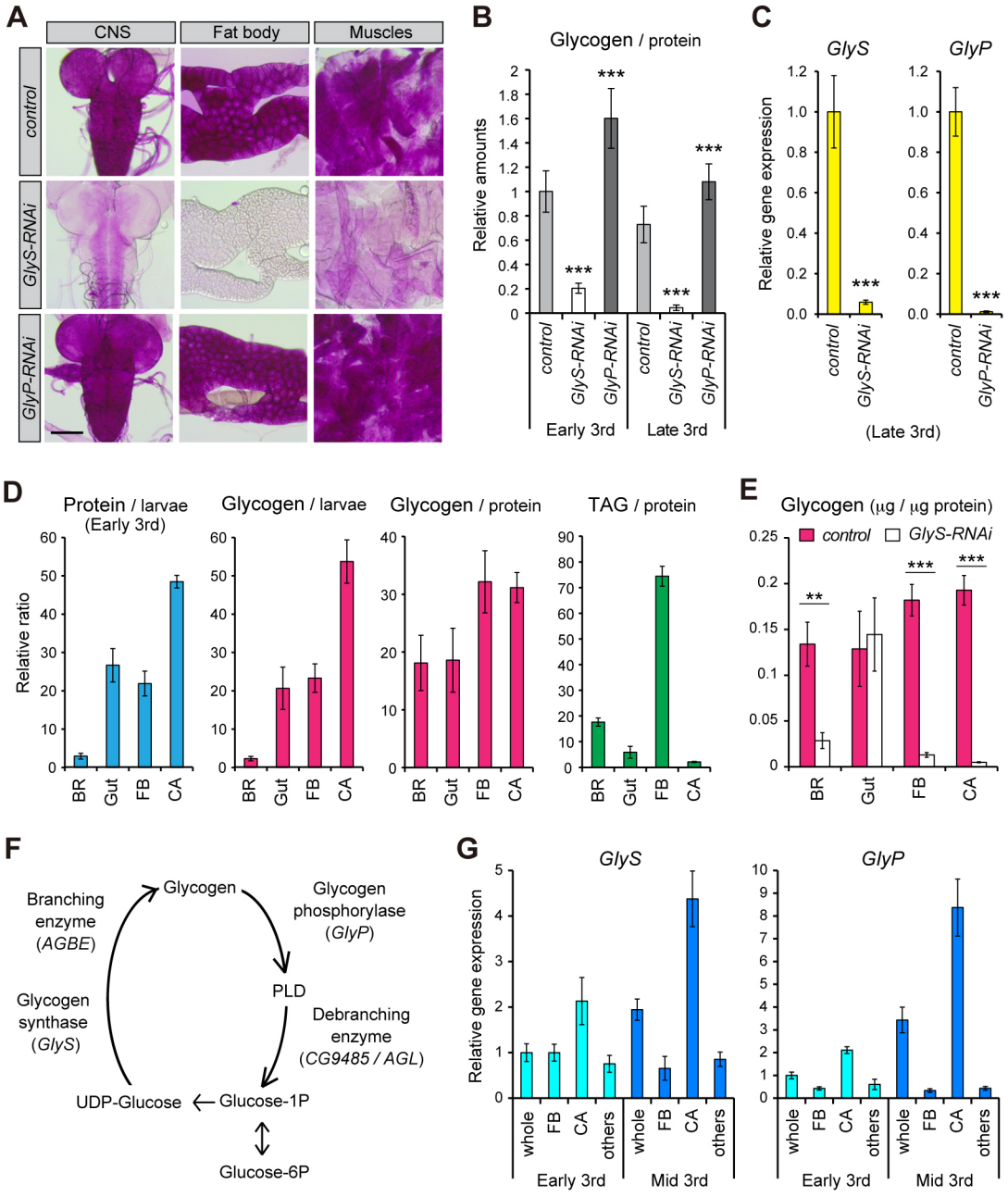

© 2018. Published by The Company of Biologists Ltd | Development (2018) 145, dev158865. doi:10.1242/dev.158865

RESEARCH ARTICLE

Fat body glycogen serves as a metabolic safeguard for the maintenance of sugar levels in *Drosophila*

Takayuki Yamada, Okiko Habara, Hitomi Kubo and Takashi Nishimura*

ABSTRACT

Adapting to changes in food availability is a central challenge for survival. Glucose is an important resource for energy production, and therefore many organisms synthesize and retain sugar storage molecules. In insects, glucose is stored in two different forms: the disaccharide trehalose and the branched polymer glycogen. Glycogen is synthesized and stored in several tissues, including in muscle and the fat body. Despite the major role of the fat body as a center for energy metabolism, the importance of its glycogen content remains unclear. Here, we show that glycogen metabolism is regulated in a tissue-specific manner under starvation conditions in the fruit fly *Drosophila*. The mobilization of fat body glycogen in larvae is independent of Adipokinetic hormone (Akh, the glucagon homolog) but is regulated by sugar availability in a tissue-autonomous manner. Fat body glycogen plays a crucial role in the maintenance of circulating sugars, including trehalose, under fasting conditions. These results demonstrate the importance of fat body glycogen as a metabolic safeguard in *Drosophila*.

KEY WORDS: *Drosophila*, Glycogen, Trehalose, Insulin, Glucagon, Fat body

INTRODUCTION

Adaptation to changes in food availability is a central challenge for survival. Both vertebrates and invertebrates have developed diverse physiological strategies to address both chronic and acute nutrient shortages. The primary strategy for survival in the absence of nutrients involves hormonal regulation and metabolic adaptation in both non-cell-autonomous and cell-autonomous manners (Unger, 1971; Saltiel and Kahn, 2001; Chng et al., 2017; Petersen et al., 2017). After feeding, circulating sugar derived from the diet is taken up by cells and used to produce energy through glycolysis. Excess glucose in the circulation can be stored as glycogen in several tissues. Glycogen is a branched polymer of glucose that serves as a form of carbohydrate energy storage in animal cells (Roach et al., 2012).

Glycogen metabolism is controlled by two enzymes, glycogen synthase and glycogen phosphorylase, the latter of which catalyzes the rate-limiting cleavage of glucose monomers from the end of a glycogen branch. The post-translational mechanism that regulates glycogen metabolism has been well characterized in mammals (Bouskila et al., 2010; Roach et al., 2012). Phosphorylation of glycogen phosphorylase by phosphorylase kinases at the conserved N-terminal serine residue leads to the activation of the enzyme by inducing a conformation change into the active state. In addition to phosphorylation, an increase in adenosine monophosphate (AMP) levels allosterically activates glycogen phosphorylase by changing its conformation. These regulatory systems are the primary mechanism by which the energy status and endocrine hormones, including glucagon, promote glycogen mobilization. Similarly, glycogen synthase is regulated by both allosteric control and phosphorylation at its N- and C-terminal domains. Phosphorylation by several kinases, including the glycogen synthase kinase 3 (GSK3) isoforms, induces inactivation of the enzyme by reducing the activity toward uridine diphosphate glucose (UDP-glucose). High levels of glucose-6-phosphate (G6P) allosterically activate glycogen synthase even when the enzyme is phosphorylated.

In mammals, muscle glycogen and liver glycogen store sugar in different physiological contexts (Roach et al., 2012; Petersen et al., 2017). Glycogen stored in muscles is directly utilized in muscle cells themselves to produce adenosine triphosphate (ATP) energy through glycolysis. On the other hand, glycogen stored in the liver is mainly utilized as a source of blood glucose for use throughout the body, including in the central nervous system (CNS). Therefore, the liver maintains a constant concentration of glucose in circulation through the glucose cycle. The difference arises from the liver-specific expression of glucose-6-phosphatase, which produces free glucose derived from glycogen.

Drosophila genetics has proven to be a powerful model system for investigating metabolic regulation at the level of the organism (Baker and Thummel, 2007; Teleman, 2009; Droujinine and Perrimon, 2016). The tissue-specific functions of glycogen in muscle and in the brain have been analyzed previously in *Drosophila* (Zirin et al., 2013, 2015; Duran et al., 2012; Saez et al., 2014; Sinadinos et al., 2014). In adults, glycogen is located in both flight muscles and the fat body (Wigglesworth, 1949; Eanes et al., 2006). The presence of glycogen in the larval fat body, however, is controversial. It has been reported that glycogen is mainly detected in body wall muscles and present at much lower levels in the fat body of a larva during feeding (Ruaud et al., 2011; Zirin et al., 2013). A recent report has demonstrated that glycogen synthesis in the fat body occurs in the late larval stage (Garrido et al., 2015). The insect fat body is widely recognized as an equivalent organ to the mammalian liver and adipose tissue (Arrese and Soulages, 2010; Leopold and Perrimon, 2007). Despite the major role of the fat body as a center for metabolic homeostasis and systemic growth regulation, the importance of fat body glycogen in *Drosophila* remains unclear.

In addition to glycogen, insects maintain a high concentration of the nonreducing disaccharide trehalose in circulating hemolymph (Becker et al., 1996; Shukla et al., 2015). Trehalose, which consists of two glucose monomers, is synthesized in the fat body and released into the hemolymph. Similar to glycogen metabolism, trehalose metabolism is governed by two enzymes: the trehalose

Laboratory for Growth Control Signaling, RIKEN Center for Developmental Biology, 2-2-3 Minatojima-Minamimachi, Chuo-ku, Kobe, Hyogo 650-0047, Japan.

*Author for correspondence (t-nishimura@cdb.riken.jp)

T.N., 0000-0002-6773-0302

Received 29 August 2017; Accepted 9 February 2018

Development (2018) 145, dev158865. doi:10.1242/dev.158865

synthesis enzyme Tps1 and the trehalose hydrolase Treh (Elbein et al., 2003). Although both trehalose and glycogen are glucose storage molecules in the *Drosophila* body, it remains unclear how the two distinct, commonly used sources are utilized to cope with nutrient shortages.

In the present study, we evaluate the tissue distribution of glycogen in larvae. Our results highlight that the tissue-specific regulation of glycogen metabolism in the fat body contributes to a metabolic safeguard for energy production. Our results also show the analogous function of the fat body and the mammalian liver in terms of the homeostatic control of circulating sugar levels. The difference is that in *Drosophila*, glycogen in the fat body is likely converted to trehalose in addition to the direct release of glucose into the circulating hemolymph.

RESULTS

Evaluation of the tissue distribution of glycogen during the larval period

To visualize glycogen stored in larval tissues, we first employed the histological method of periodic acid–Schiff (PAS) staining, which detects polysaccharides including glycogen. Using whole-mount PAS staining, we detected strong signals in several tissues of mid third-instar larvae (Fig. 1A). The PAS staining was almost completely abolished by the ubiquitous knockdown of *GlyS* in tissues, such as the CNS, fat body and body wall muscles. These results indicate that PAS staining visualizes glycogen in these tissues with high fidelity. On the other hand, the knockdown of *GlyS* decreased the PAS signals partially, but not completely, in the imaginal discs, midgut, Malpighian tubules, testes and ovaries (Fig. S1A). The strong signal in the salivary glands was not changed after the knockdown of *GlyS*. Therefore, these tissues contain PAS stain-positive polysaccharides other than glycogen, which made it difficult to evaluate the level of stored glycogen.

To further validate the distribution of glycogen during the larval period, we quantified glycogen based on an enzymatic assay for glucose after digestion of the glycogen polymer with amyloglucosidase (Tennessen et al., 2014). The ubiquitous knockdown of *GlyS* reduced the glycogen level (defined herein as the free glucose level after enzyme digestion) markedly, but did not eliminate it completely, whereas the knockdown of *GlyP* increased the glycogen level in whole larvae (Fig. 1B). Notably, we failed to recognize a ∼1.5-fold increase in glycogen in the *GlyP* knockdown larvae by PAS staining under these conditions (Fig. 1A). The knockdown efficiencies of *GlyS* and *GlyP* were confirmed by qPCR (Fig. 1C). We next evaluated the glycogen contents of individual tissues in early third-instar larvae. Glycogen was mainly detected in the carcass, which includes the epidermis and the body wall muscles of the larvae (Fig. 1D). Glycogen was also detected in the fat body, gut and CNS. Importantly, the content of glycogen in the fat body was almost equivalent to that in the carcass after normalization to the protein level in each tissue. On the other hand, triglyceride (TAG) was mainly distributed in the fat body under these conditions. We next assessed the specificity of the signals obtained by the enzymatic assay. The ubiquitous knockdown of *GlyS* resulted in a significant reduction in glycogen in the carcass, fat body and CNS (Fig. 1E), which is consistent with the results obtained by PAS staining. On the other hand, there was no clear difference in the midgut between the control and *GlyS* knockdown larvae in the early third instar, suggesting that the quantification of glycogen by an enzymatic assay contains a certain degree of background signal that is most likely derived from dietary polysaccharides in the midgut. This possibility is reasonable because amyloglucosidase, which is widely utilized for the digestion of glycogen, also digests starch and maltose. Consistently, the knockdown of *GlyS* reduced the glycogen level further in the wandering late third instar, in which the gut contents are excreted for pupariation, compared with the early third instar (Fig. 1B). Together, these results suggest that not only the body wall muscles but also other tissues, including the fat body, synthesize and store glycogen. In this work, we mainly focused on the body wall muscles, fat body and CNS for further analyses because of the reliability of the PAS staining and enzymatic assay for quantification.

We next examined the transcript levels of genes involved in glycogen metabolism (Fig. 1F). *GlyS* and *GlyP* were expressed in both the body wall muscles and the fat body in the early third instar (Fig. 1G). Consistently, the glycogen branching enzyme *AGBE* and de-branching enzyme *AGL* (*CG9485*) were expressed in various tissues including the fat body (Fig. S1B). It has been reported that *GlyS* expression is detected in body wall muscles and is undetectable in the larval fat body, as determined using a transposon insertion line that directs GFP expression under the control of the *GlyS* regulatory element (Zirin et al., 2013). Consistent with the previous report, we observed that GFP expression in a reporter line, *Minos* insertion $GlyS^{MI01490}$, was high in muscles and low in the fat body (Fig. S2A). However, a homozygous mutation of $GlyS^{MI01490}$ abolished the PAS staining in the body wall muscles and CNS, but not in the fat body (Fig. S2B,C). It appears that $GlyS^{MI01490}$ disrupts several *GlyS* transcripts (*RB*, *RC* and *RD*), but one transcript, *GlyS-RA*, is fully intact (Fig. S2D). Taking into account the fact that $GlyS^{MI01490}$ failed to disrupt the function of *GlyS* in the fat body, it is possible that *GlyS-RA* is expressed in the fat body. As expected, *GlyS-RA* was predominantly expressed in the fat body (Fig. S2E,F). Together, these results indicate that GFP expression in $GlyS^{MI01490}$ does not recapitulate all transcription from the *GlyS* gene locus, especially in the fat body.

Starvation induces the complete breakdown of glycogen in the fat body

Storage sugars are utilized as energy sources for survival during fasting. Therefore, we next analyzed the decay kinetics of storage sugars after starvation using a biochemical method at the level of whole larvae. A reduction of glycogen was observed within 1 h of starvation in early third-instar larvae (Fig. 2A). Subsequently, the amount of glycogen gradually reduced in a linear manner up to 4 h and reached ∼30% of the original. Then, the reduction rate of glycogen became slow and reached ∼10% of the original value at 24 h after starvation. By contrast, the amount of trehalose remained at the same level after up to 2 h of starvation. The reduction of trehalose became significant at 4 h after starvation and reached ∼10% of the original value at 24 h after starvation. Under these conditions, the amount of free glucose gradually decreased during starvation and reached ∼50% of the original value after 24 h of starvation.

Because liver glycogen and muscle glycogen are utilized for different purposes in mammals, we next asked whether the mobilization of glycogen under starvation is regulated differently between organs. We found that glycogen in the fat body decreased shortly after the onset of starvation and completely disappeared after 4 h of starvation (Fig. 2B,C). The body wall muscles, but not the CNS, lost glycogen during starvation but retained a certain amount of glycogen even after 3 days of starvation (Fig. 2B). In agreement with the PAS staining results, starvation led to the complete breakdown of fat body glycogen as visualized by immunostaining

Development (2018) 145, dev158865. doi:10.1242/dev.158865

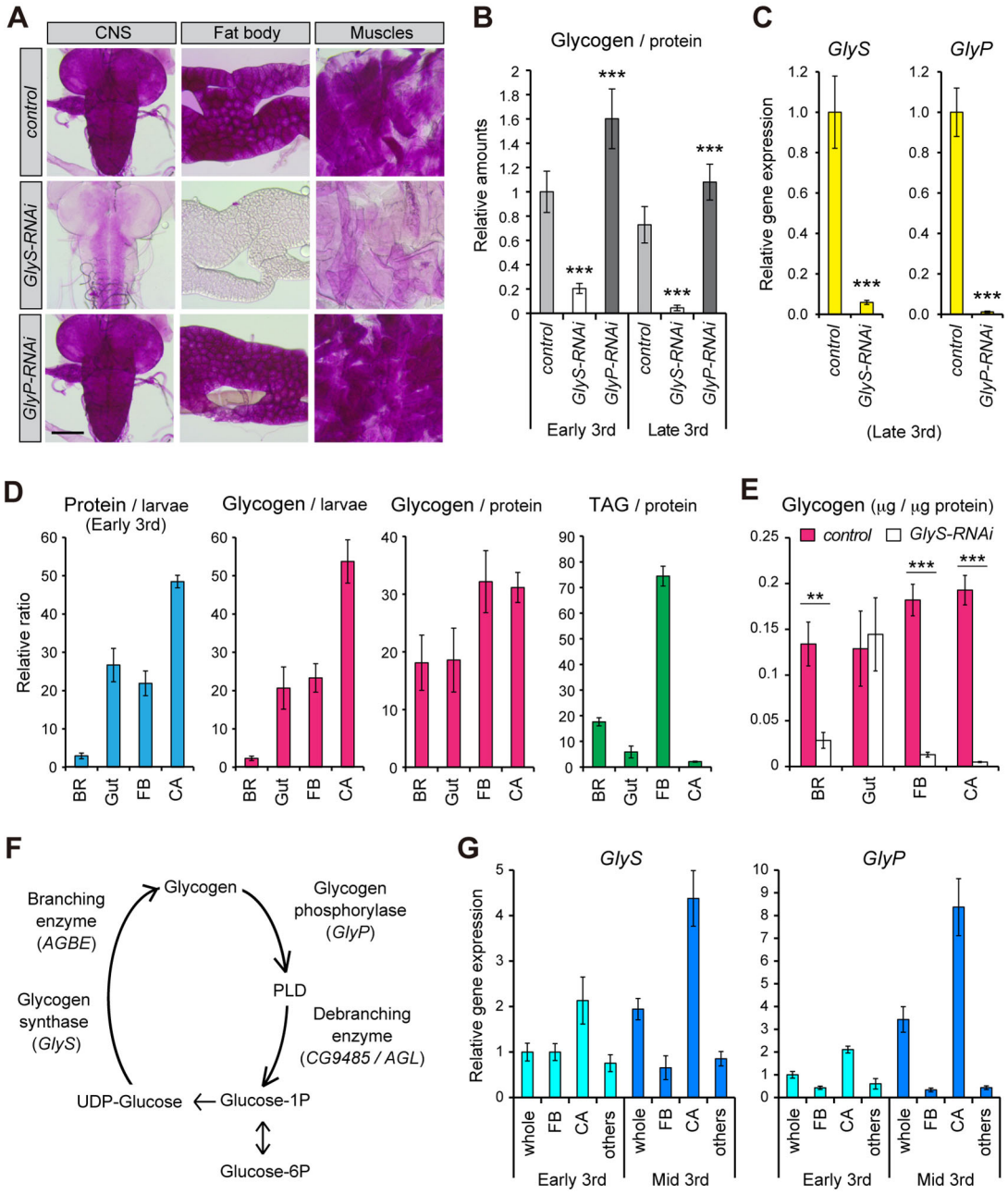

Fig. 1. Validation of PAS staining and biochemical quantification of glycogen in *Drosophila* larval tissues. (A) Tissue distribution of stored glycogen was assessed by PAS staining in mid third-instar larvae. Ubiquitous knockdown of *GlyS*, but not of *GlyP*, by *tub-Gal4* produced a significant reduction in PAS signals in each organ as shown. CNS, central nervous system; Muscles, body wall muscles. Scale bar: 100 µm. (B) The total amounts of glycogen were analyzed in early or late third-instar larvae of the indicated genotypes. (C) Knockdown of *GlyS* and *GlyP* was confirmed by qRT-PCR in late third-instar larvae. (D) Tissue distributions of protein, glycogen and TAG were analyzed by a biochemical quantification method in the early third instar of the wild-type larvae. The amounts of protein and glycogen are shown as values per larva or values normalized to the protein levels in each tissue. The total values were set to 100, and the relative levels in each tissue are shown. BR, central nervous system and imaginal discs; Gut, midgut; FB, fat body; CA, carcass including body wall muscles. (E) The specificity of the biochemical quantification of glycogen was assessed in early third-instar larvae. The amounts of glycogen normalized to the protein level in each tissue are shown. (F) Genes involved in glycogen synthesis and mobilization. PLD, phosphorylase-limit dextrin. (G) Tissue distributions of *GlyS* and *GlyP* transcripts were analyzed by qRT-PCR in early third-instar and mid third-instar larvae. whole, whole larva; FB, fat body; CA, carcass including body wall muscles; others, midgut and CNS. Values shown are means±s.d. n=3 (C,E), n=4 (G) or n=6 (B,D). $^{**}P<0.01$, $^{***}P<0.001$; one-way ANOVA with Dunnett's post hoc test (B) or two-tailed Student's t-test (C,E).

with a monoclonal anti-glycogen antibody (Fig. 2D). The knockdown of *GlyS* reduced PAS signals in muscles and the CNS to a greater extent than starvation conditions (Fig. 1A), indicating that the remaining glycogen is present in tissues other than the fat body. These observations were confirmed by biochemical quantification (Fig. 2E). There was only a minor change in brain glycogen, while ∼20% of glycogen was maintained in the body wall muscles after 2 days of starvation. In contrast to sugar storage, the stored TAG in the fat body, visualized by Oil Red O staining, decreased gradually for a few days after starvation and eventually disappeared (Fig. 2B). It has been reported that a defect in fatty acid synthesis in the fat body results in an increased glycogen content

Development (2018) 145, dev158865. doi:10.1242/dev.158865

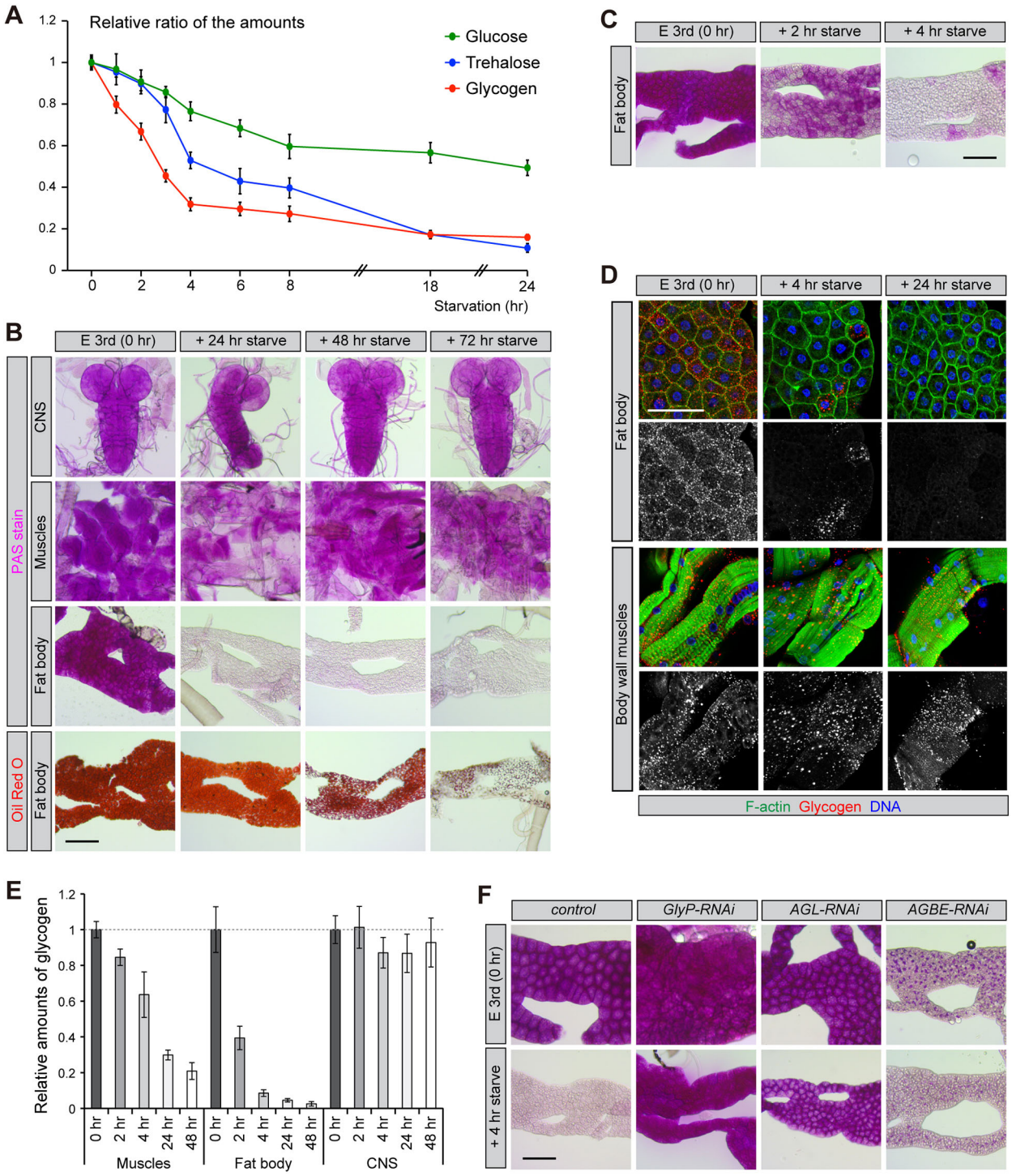

Fig. 2. Glycogen is consumed in a tissue-dependent manner under starvation. (A) Relative changes in the amounts of glucose, trehalose and glycogen under starvation conditions. Wild-type early third-instar larvae grown on normal food (0 h) were transferred and cultured on agar food (starved) for the indicated times. The initial amount of each metabolite was set to 1. (B) Stored glycogen in each tissue was visualized by PAS staining under starvation conditions. Lipid droplets including TAG in the fat body were visualized by Oil Red O staining. Early third-instar larvae (E 3rd) were used for the experiments. (C) Fat body glycogen was consumed 4 h after starvation. (D) Mobilization of fat body glycogen under starvation. Glycogen in the fat body or body wall muscles was immunostained with anti-glycogen antibodies. (E) Relative amounts of glycogen in each organ were analyzed by biochemical quantification. The hours indicate the duration of the starvation period from the early third instar. (F) Knockdown of *GlyP* and *AGL* disrupts the degradation of fat body glycogen under starvation, whereas the knockdown of *AGBE* causes punctate aggregation of glycogen. *CG-Gal4* was used for fat body-specific knockdown. Values shown are means±s.e.m. n=6 (A) or n=4 (E). Scale bars: 100 µm.

(Parvy et al., 2012; Garrido et al., 2015). By contrast, both the lipogenesis and mobilization of TAG in the fat body appeared to be independent of glycogen metabolism, because the loss of fat body glycogen had no significant impact on the steady-state level or mobilization of TAG (Fig. S3A). The accumulation of lipid droplets in oenocytes serves as an indicator of lipid mobilization in the fat

Development (2018) 145, dev158865. doi:10.1242/dev.158865

body (Gutierrez et al., 2007). The accumulation of lipid droplets in oenocytes occurred in *GlyS* knockdown larvae under fasting conditions, similar to the control larvae (Fig. S3B), indicating that lipid mobilization from the fat body is not affected by the absence of fat body glycogen. It should be noted that a more than 50% reduction of glycogen in the muscles was detected by the enzymatic assay after starvation (Fig. 2E). However, it is sometimes difficult to visualize such a 50% reduction in the body wall muscles using the PAS staining and anti-glycogen antibody signals (Fig. 2B,D). The exact reason remains unclear, but these staining methods might be too intense for identifying such a difference in muscle glycogen.

To further confirm the mobilization of glycogen, we next analyzed the function of *GlyP*. As expected, the knockdown of *GlyP* completely abolished the mobilization of glycogen in the fat body (Fig. 2F). We obtained similar results by knocking down the de-branching enzyme *AGL*. By contrast, knocking down the branching enzyme *AGBE* caused large aggregates that were visible by the PAS staining (Fig. 2F, Fig. S4A,B). It appears that the long unbranched glucose chains have a low solubility, which results in glycogen aggregation in the cytoplasm. Nevertheless, this precipitated glycogen largely disappeared from the fat body after starvation. Taken together, these results revealed that the mobilization of glycogen under starvation is tightly regulated in a tissue-specific manner.

Mobilization of fat body glycogen under starvation is independent of Akh

It has been reported that an adipokinetic hormone called Akh regulates the mobilization of glycogen under starvation conditions in *Drosophila*, similar to the action of glucagon in mammals (Kim and Rulifson, 2004; Lee and Park, 2004; Gáliková et al., 2015). In addition, its receptor, AkhR, is highly expressed in the fat body (Grönke et al., 2007; Bharucha et al., 2008). Because of the high sequence similarities, including the phosphorylation sites, between species in glycogen synthase and phosphorylase (Fig. S5), it is reasonable to assume that the regulatory system of enzyme activity is highly conserved in *Drosophila*. These observations prompted us to examine whether Akh regulates glycogen mobilization in the fat body under fasting conditions. To test this, we genetically ablated the corpora cardiaca (CC) endocrine cells, which secrete Akh, through the induction of the pro-apoptotic genes *rpr* and *grim* (Kim and Rulifson, 2004). However, even in the absence of CC, the breakdown of glycogen in the fat body occurred normally after starvation (Fig. 3A, Fig. S6A). We confirmed the significant reduction in the *Akh* expression levels by inducing the pro-apoptotic genes (Fig. 3B). These results suggest that CC cells, which generate Akh, are not involved in the mobilization of glycogen under these conditions. Furthermore, neither the ectopic expression of *Akh* in the CC cells nor in the fat body affected the steady-state level or the reduction of glycogen in the fat body upon starvation, as judged by the PAS signals (Fig. 3A,C). Similar results were observed in the muscle glycogen (Fig. 3C). We next attempted to knock down *AkhR* in the fat body. However, the knockdown of *AkhR* did not affect the steady-state level or the reduction of glycogen upon starvation (Fig. 3D, Fig. S7).

To further confirm the independence of Akh signal in glycogen metabolism, we next analyzed null mutants of *Akh* and *AkhR* (Grönke et al., 2007; Gáliková et al., 2015). Consistently, both the *Akh* and *AkhR* null mutants showed no defects regarding the steady-state level or mobilization of glycogen in the fat body upon starvation (Fig. 3E, Fig. S6B). These results demonstrate that glycogen metabolism in the larval fat body is regulated in an Akh-independent manner.

Breakdown of glycogen in the fat body is regulated tissue autonomously

The enzymatic activity of GlyP is regulated not only by phosphorylation that is stimulated by hormones but also in an allosteric manner (Roach et al., 2012). The increase in cellular AMP levels is known to activate GlyP, while high concentrations of G6P suppress GlyP. Therefore, the reduction in energy levels in forms such as ATP and glucose under starvation conditions might directly activate GlyP to break down glycogen. To understand the mechanism of the mobilization of fat body glycogen, we next analyzed the dietary conditions that trigger the breakdown of glycogen. We found that providing dietary glucose was sufficient to block the breakdown of glycogen in the fat body (Fig. 4A). On the other hand, if the larvae were transferred from a standard diet to a yeast-only or cornflour-only diet, the complete breakdown of fat body glycogen was observed 4 h after the dietary change. However, continuous feeding of a yeast-only or cornflour-only diet for 1 day restored the fat body glycogen eventually. A feedback regulatory system called glucose suppression operates to limit the digestion of carbohydrates (Chng et al., 2017). In *Drosophila*, dietary glucose negatively regulates the expression of secreted enzymes in the midgut that digest dietary polysaccharides. Therefore, we speculated that digestive enzymes are suppressed under a normal diet, which contains a high concentration of glucose. Consistent with this hypothesis, the fat body glycogen was depleted transiently when the larvae were transferred from a standard diet to a maltose-only or starch-only diet (Fig. 4A). We further found that the expression of maltase genes, such as *Mal-A2*, *Mal-A3* and *Mal-A4*, was upregulated transiently 4 h after the dietary change to a maltose-, starch- or cornflour-only diet (Fig. 4B, Fig. S8). Continuous feeding of an agar-only or yeast-only diet failed to suppress the maltase expression, resulting in further induction. By contrast, the expression of an amylase, *Amy-p*, was upregulated strongly by the feeding of an agar-only, starch-only or yeast-only diet. It seems that the expression of maltase, which acts downstream in the process of carbohydrate digestion, is more sensitive than that of amylase to a change in dietary carbohydrate conditions. These results strongly support the idea that the removal of free glucose from the diet stimulates the expression of maltase for the digestion of dietary carbohydrates, which probably takes several hours. This time lag results in a transient shortage of glucose in the body, which triggers the mobilization of fat body glycogen.

We next asked whether dietary glucose is sufficient to restore the fat body glycogen. As expected, re-feeding glucose for 4 h after starvation was sufficient to restore the glycogen content in the fat body, similar to the effect of re-feeding a normal diet (Fig. 4C). Intriguingly, such fluctuation in the glycogen content was not observed in the CNS (Fig. 4A,C), indicating that the fat body glycogen is highly sensitive to dietary conditions. Together, these results suggest that dietary sugar is important for both the maintenance and restoration of fat body glycogen on a short-term basis.

To further obtain insights into the mobilization of fat body glycogen, we conducted *ex vivo* organ culture experiments. If the dissected fat body from early third-instar larvae was cultured in PBS, a reduction of glycogen was observed 4 h after incubation (Fig. 4D), just as it was 4 h after starvation *in vivo*. By contrast, the reduction of glycogen was completely suppressed by incubation in either Schneider's *Drosophila* medium or Dulbecco's modified Eagle medium (DMEM) (data not shown). We found that the addition of glucose, but not of bovine serum albumin (BSA), to PBS was sufficient to block the degradation of glycogen in a dose-dependent

Development (2018) 145, dev158865. doi:10.1242/dev.158865

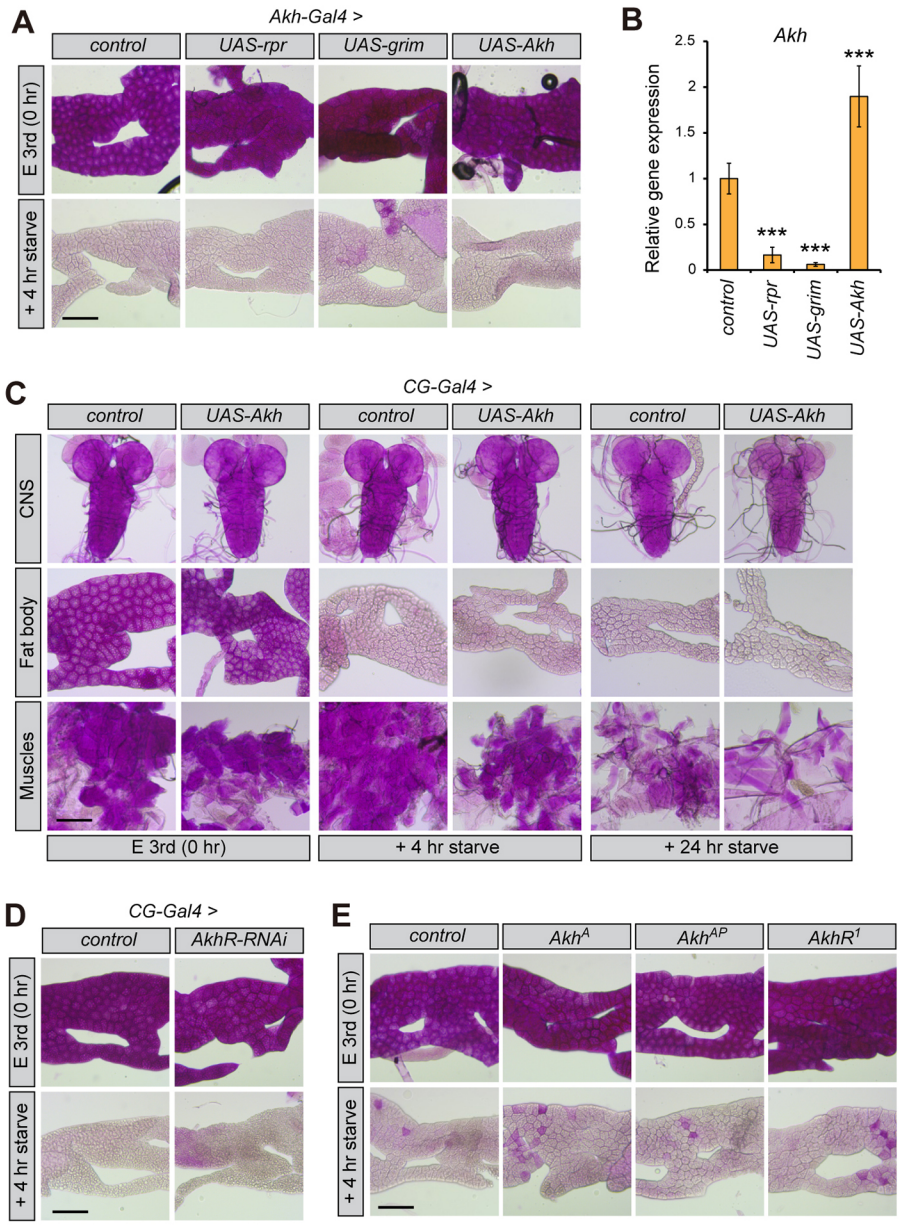

Fig. 3. Mobilization of fat body glycogen is independent of the Akh signal. (A) Loss of Akh-producing cells and overexpression of *Akh* in the Akh-producing cells have no impact on the steady-state levels or mobilization of fat body glycogen. Fat body glycogen was analyzed by PAS staining in early third-instar larvae (E 3rd) and after 4 h of starvation. (B) Genetic ablation of the Akh-producing cells was confirmed by qRT-PCR in early third-instar larvae. The values shown are means± s.d. (n=4). ***P<0.001; one-way ANOVA with Dunnett's post hoc test. (C) The overexpression of *Akh* in the fat body does not affect the steady-state levels or mobilization of glycogen in any organ. (D) Knockdown of *AkhR* in the fat body does not affect the steady-state levels or mobilization of fat body glycogen. (E) *Akh* and *AkhR* null mutants have no defects in their steady-state levels or mobilization of fat body glycogen in early third-instar larvae. Scale bars: 100 µm.

manner. 2-Deoxyglucose (2DG) was more potent in blocking the degradation of glycogen. 2DG is converted to 2-deoxyglucose-6-phosphate (2DG6P) and acts as a glycolytic inhibitor. Therefore, 2DG6P likely suppresses the activity of GlyP, similar to G6P. Furthermore, glucose in the culture medium was sufficient to restore the fat body glycogen in a dose-dependent manner when the fat body was dissected from starved larvae (Fig. 4E). These results demonstrate that the mobilization and restoration of glycogen in the fat body occurs in *ex vivo* conditions without any other organs, and that glycogen metabolism can be regulated by the availability of glucose in a tissue-autonomous manner.

Insulin/insulin-like growth factor signaling facilitates glycogen synthesis in the fat body

In contrast to the role of Akh/glucagon in glycogen mobilization, insulin/insulin-like growth factor (IGF) signaling (IIS) regulates glycogen synthesis (Roach et al., 2012; Chng et al., 2017). To investigate the impact of IIS on glycogen metabolism, we next analyzed the function of InR in the fat body. The knockdown of *InR* in the fat body using *CG-Gal4* caused no significant defect in the glycogen level of the early third-instar larvae or in the mobilization upon starvation (Fig. 5A). Because it is difficult to distinguish the effects of IIS on the synthesis and degradation of glycogen from any of the effects on the steady-state level, we next analyzed the restoration rate of glycogen after starvation. The knockdown of *InR* in the fat body produced a significant delay in the restoration of fat body glycogen after starvation (Fig. 5A). Consistently, *ex vivo* organ culture experiments revealed the necessity of IIS for the recovery of glycogen in the fat body. Importantly, glucose uptake as revealed by a fluorescently labeled deoxyglucose, 2-[*N*-(7-nitrobenz-2-oxa-1,3-diazol-4-yl)amino]-2-deoxyglucose (2-NBDG), was not affected by the knockdown of *InR* in the fat body. Because there was no external ligand for InR in our *ex vivo* culture experiments, we analyzed the expression levels of genes involved in glycogen metabolism. The expression levels of *GlyS*, *GlyP* and *AGL* were

Development (2018) 145, dev158865. doi:10.1242/dev.158865

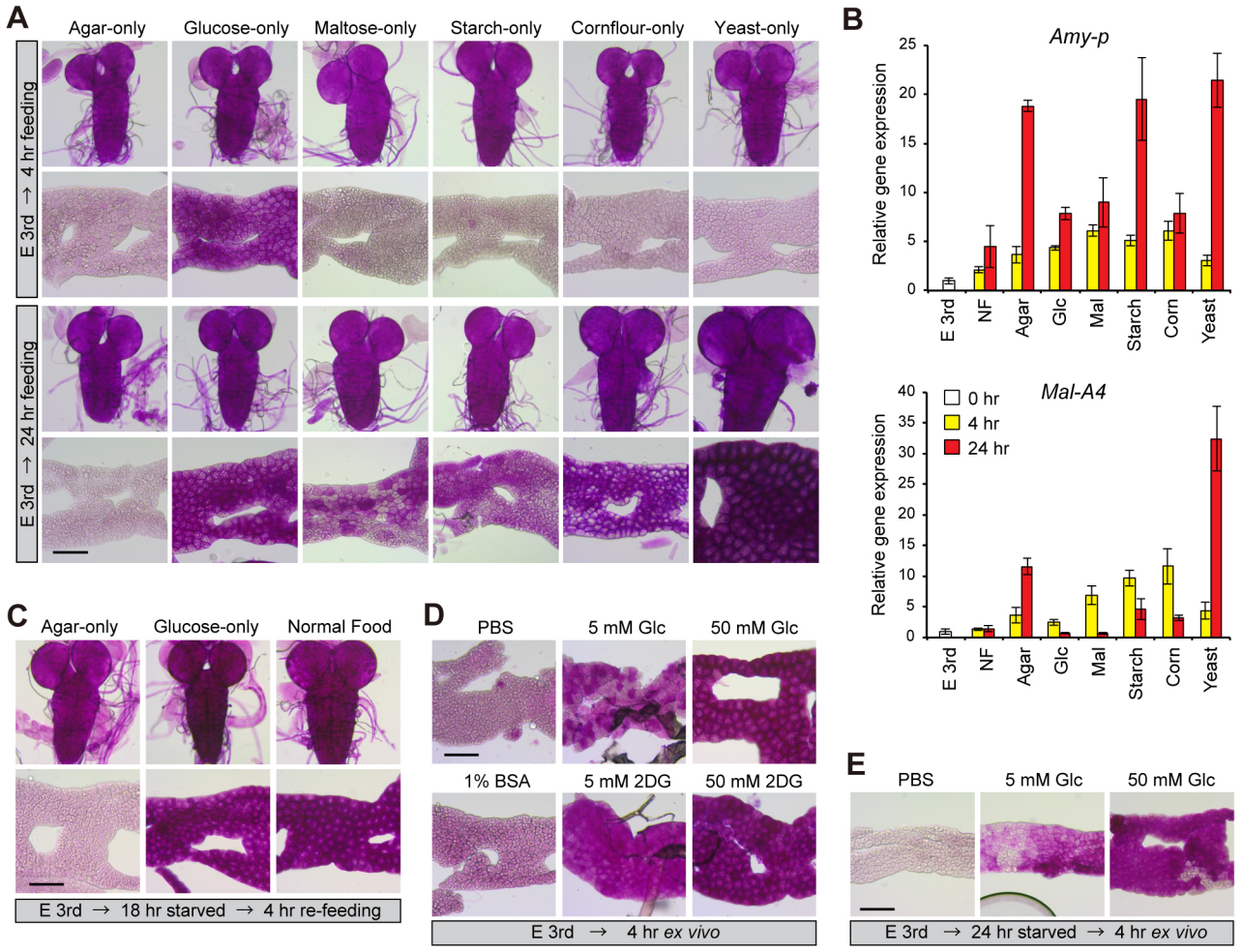

Fig. 4. Mobilization of fat body glycogen is mainly regulated by the sugar level. (A) Dynamic change in fat body glycogen depending on dietary conditions. Wild-type early third-instar larvae (E 3rd) grown on normal food were cultured under the indicated dietary conditions. Fat body glycogen and brain glycogen were analyzed at 4 h or 24 h after transfer. Notably, the yeast-only diet promoted growth in the brain and the fat body. (B) Changes in the expression levels of digestive enzymes, *Amy-p* and *Mal-A4*, under various dietary conditions. The expression levels were analyzed by qRT-PCR. NF, normal food; Glc, glucose; Mal, maltose; Corn, cornflour. Values shown are means±s.d. (n=3). (C) Glucose-only diet was sufficient for a full recovery of fat body glycogen after starvation. The CNS and the fat body were dissected at 4 h after the re-feeding of the indicated diet. (D) Glucose is sufficient for the maintenance of fat body glycogen *ex vivo*. Dissected fat bodies from early third-instar larvae were cultured for 4 h in medium as indicated. Glc, glucose; 2DG, 2-deoxyglucose. (E) Fat body glycogen was recovered under *ex vivo* culture conditions in a glucose dose-dependent manner. Fat bodies dissected from starved early third-instar larvae were used for the experiment. Scale bars: 100 µm.

significantly reduced in the fat body (Fig. 5B). These changes were specific because the expression levels of the trehalose synthesis enzyme *Tps1* and the trehalose transporter *Tret1-1* did not change under these conditions. These results suggest that IIS regulates the ability of glycogen synthesis following glucose uptake in the fat body. Although *GlyP* expression was downregulated under these conditions, we failed to observe the defects in glycogen mobilization (Fig. 5A). Because IIS negatively regulates the enzyme activity of GlyP through the activation of PP1 proteins (Roach et al., 2012), the reduced expression level of *GlyP* might be compensated by the increased enzyme activity.

We further examined the effects of IIS on glycogen metabolism. The synthesis of glycogen in the fat body was enhanced in the presence of bovine insulin *in vitro* (Fig. 5C), indicating that IIS stimulates glycogen synthesis in the fat body. Consistently, the overexpression of a constitutively active PI3K (Pi3K92E – FlyBase; *UAS-p110-CAAX*) partially blocked the reduction of glycogen under starvation conditions (Fig. 5D). PI3K blocks the formation of autophagy in the fat body (Scott et al., 2004). It has been reported that a portion of the glycogen content is degraded through autophagy in *Drosophila* body wall muscles (Zirin et al., 2013). However, this degradation is unlikely in the fat body, given that the inhibition of autophagy using dominant-negative Atg1 (*UAS-Atg1-KQ*) failed to block the mobilization of fat body glycogen under starvation (Fig. 5D). We also failed to detect the colocalization of glycogen and lysosomes in the fat body (Fig. 5E). Taken together, these results demonstrate that IIS can facilitate glycogen synthesis in the fat body.

Fat body glycogen is required to maintain trehalose levels under starvation

Our observations demonstrate that the reduction rate of glycogen is faster than that of trehalose shortly after starvation. The fat body is the sole site of trehalose synthesis (Matsuda et al., 2015). Therefore, glycogen in the fat body can be utilized for the synthesis of trehalose as a source of glucose under starvation. If this is the case, the amount

Development (2018) 145, dev158865. doi:10.1242/dev.158865

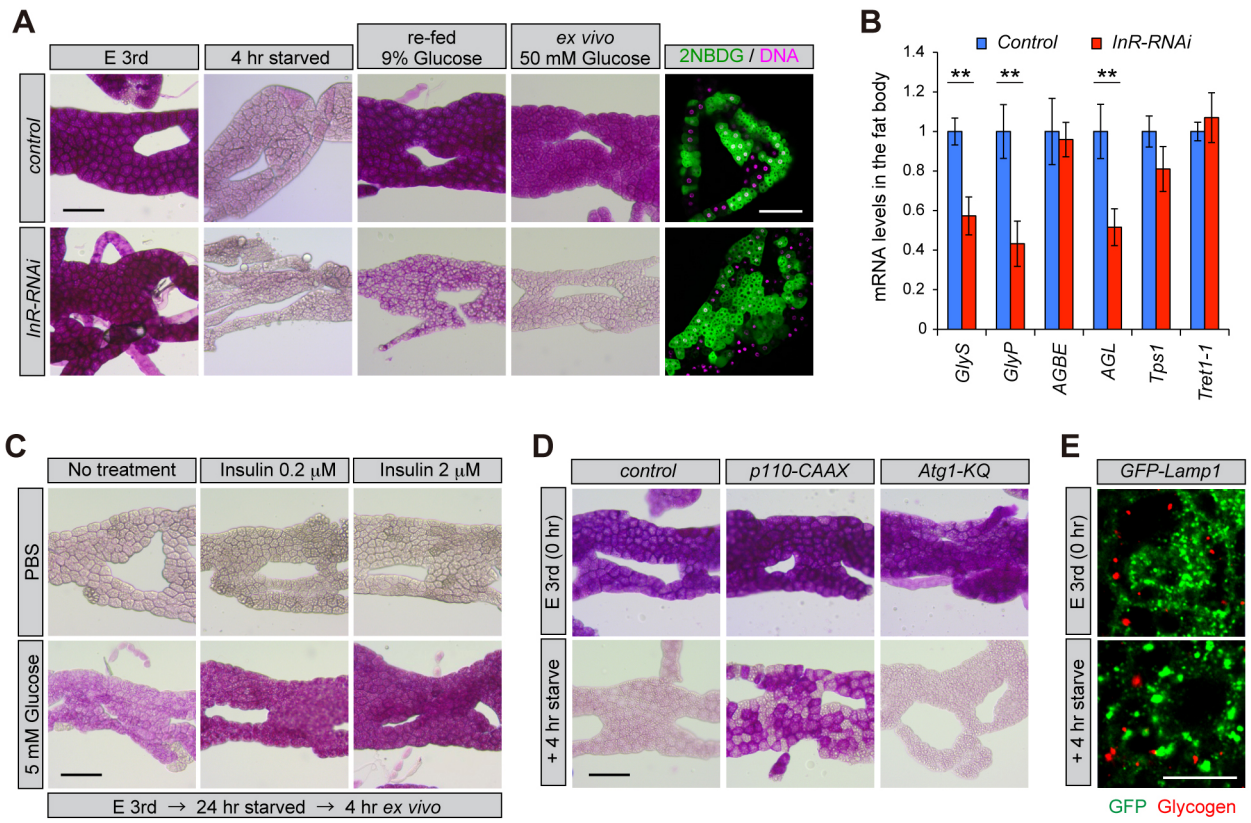

Fig. 5. Insulin signaling facilitates the synthesis of fat body glycogen. (A) Knockdown of *InR* in the fat body reduced the recovery rate of fat body glycogen after starvation but did not affect the steady-state levels under fed conditions. Fat body glycogen was analyzed under the indicated culture conditions. Glucose uptake is not affected as tested with 2-NBDG. (B) Knockdown of *InR* in the fat body decreases the expression of *GlyS* and *GlyP*. The expression levels were analyzed by qRT-PCR in fat bodies dissected from early third-instar larvae. Values shown are means±s.d. (n=3). **P<0.01; two-tailed Student's t-test. (C) Bovine insulin facilitates the recovery of fat body glycogen after starvation in a dose-dependent manner. Fat bodies dissected from starved early third-instar larvae were used for the experiment. (D) Activation of PI3K (*p110-CAAX*), but not inhibition of autophagy (*Atg1-KQ*), partially blocks the mobilization of fat body glycogen under starvation. (E) Glycogen is not colocalized with lysosomes, as visualized with GFP-Lamp1. The remaining glycogen in the fat body was imaged under starvation conditions. Scale bars: 100 µm (A,C,D), 20 µm (E).

of trehalose will reduce after a short period of starvation in the absence of fat body glycogen. Indeed, trehalose decreased significantly after 2, 4 and 6 h of starvation when either *GlyS* or *GlyP* was knocked down specifically in the fat body (Fig. 6A). A similar decrease was detected in the glucose level after starvation, suggesting that fat body glycogen contributes to the levels of both trehalose and glucose after starvation. Notably, there were no significant differences in the steady-state trehalose or glucose levels in these larvae. In addition, the knockdown of *GlyS* in the fat body resulted in a 25% decrease in glycogen in whole larvae. The difference between control and *GlyS* knockdown larvae was observed only before and 2 h after starvation and not at 4 or 6 h after starvation. This result is consistent with the fact that the fat body glycogen is almost completely consumed after 4 h of starvation.

Because the balance between synthesis and consumption determines the steady-state level of trehalose, we next analyzed the enzyme activity of Treh before and after starvation. Treh activity in the whole larval homogenate was observed under both the fed and starvation conditions in a comparable manner (Fig. 6B), suggesting that trehalose is dynamically degraded by Treh not only under starvation conditions but also under fed conditions. Together, these results demonstrate that the maintenance of trehalose levels shortly after starvation is achieved by the supply derived from *de novo* trehalose synthesis in the fat body.

A deficit in fat body glycogen aggravates the phenotype caused by the *Tps1* mutation

We next examined the physiological relevance of fat body glycogen. Although the fat body glycogen was consumed after 4 h of starvation, the knockdown of *GlyS* in the fat body produced only a slight decrease in starvation tolerance compared with control larvae (Fig. 6C). Furthermore, the loss of the fat body glycogen did not affect larval growth as judged by pupal volume on either a standard diet or a poor diet (Fig. 6D). The knockdown of *GlyS* in the fat body did not show any lethality during development (Fig. 6E), indicating that the fat body glycogen is dispensable for body growth and viability.

Because trehalose is required for starvation tolerance and viability (Matsuda et al., 2015), we reasoned that the observed mildness or absence of the phenotype in *GlyS* knockdown flies is caused by the presence of trehalose. To test the phenotypic interaction between fat body glycogen and trehalose, we attempted to impair both glycogen metabolism and trehalose synthesis in the fat body. Consistent with the phenotype of the *Tps1* null mutants, the knockdown of *Tps1* in the fat body produced strong lethality under starvation (Fig. 6C). The observed lethality in the *Tps1* knockdown larvae is milder than that in the *Tps1* null mutants (Matsuda et al., 2015), suggesting that the *Tps1* knockdown produces a partial, but not complete, reduction of mRNA. Under these conditions, the double knockdown of *GlyS* and *Tps1*

Development (2018) 145, dev158865. doi:10.1242/dev.158865

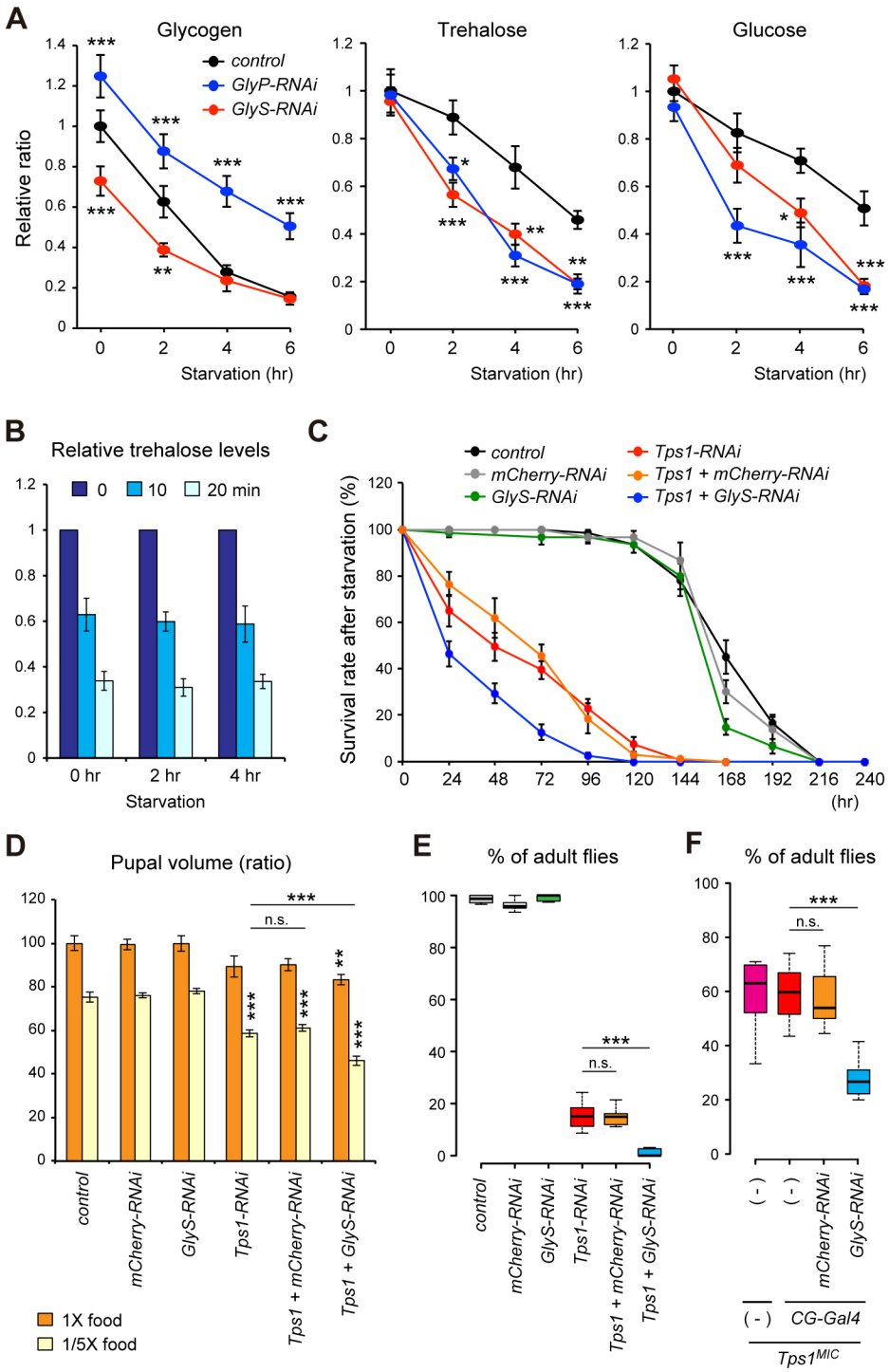

Fig. 6. Fat body glycogen is required to maintain trehalose levels under starvation. (A) Relative changes in the amounts of glucose, trehalose and glycogen under starvation conditions. Early third-instar larvae grown on normal food (0 h) were transferred and cultured on agar food (starved) for the indicated amounts of time. *CG-Gal4* was used for fat body-specific knockdown. The initial amount of each metabolite in the control was set to 1. (B) Trehalase activity was measured in wild-type larval homogenates before and after starvation. The relative levels of trehalose after the indicated incubation periods are shown. (C) Knockdown of *GlyS* in the fat body by *CG-Gal4* decreases the survival rate of *Tps1* mutants under fasting conditions. Early third-instar larvae were transferred to a vial containing 0.8% agar in PBS, and the number of surviving larvae was counted at the indicated time points. (D) Loss of fat body glycogen intensifies the decrease in body size caused by the loss of *Tps1*. Relative pupal volumes grown on a normal diet (1× food) or a low-protein diet (1/5× food) are shown. (E) Knockdown of *GlyS* in the fat body increases the pupal lethality of the *Tps1* knockdown. The percentage of adult flies was determined by the ratio of eclosed to total flies. (F) Knockdown of *GlyS* in the fat body further reduces the survival rate of mutants with the hypomorphic allele of *Tps1*, $Tps1^{MIC}$. The percentage of adult flies was determined by the ratio to flies with a balancer chromosome in each vial. The values shown are means±s.e.m. n=6 (A,E,F), n=4 (B,C) or n=30 (D). *P<0.05, **P<0.01, ***P<0.001; n.s., not significant; two-way ANOVA with Dunnett's post hoc test (A) or one-way ANOVA with Tukey's post hoc test (D-F).

significantly enhanced the lethality after starvation compared with *Tps1* knockdown or *Tps1* and *mCherry* double knockdown (Fig. 6C), indicating that the loss of fat body glycogen aggravates the phenotype of the *Tps1* mutants. Consistently, the knockdown of *GlyS*, but not of *mCherry*, enhanced the growth defects of the *Tps1* knockdown larvae (Fig. 6D).

The knockdown of *Tps1* caused pupal lethality with some escapers (Fig. 6E), as reported previously (Matsuda et al., 2015). A similar genetic interaction was observed in the rate of pupal lethality caused by *Tps1* knockdown (Fig. 6E). Furthermore, the knockdown of *GlyS*, but not of *mCherry*, in the fat body enhanced the pupal lethality of the hypomorphic allele of *Tps1* that reduces trehalose to 20% of the control levels (Fig. 6F) (Matsuda et al., 2015). Taken together, these results demonstrate that fat body glycogen serves as a metabolic safeguard for the maintenance of circulating sugar levels.

DISCUSSION

We report here that glycogen metabolism is regulated in an organ-specific manner under fasting conditions in *Drosophila*. In

Development (2018) 145, dev158865. doi:10.1242/dev.158865

particular, fat body glycogen has a unique character compared with glycogen stored in other organs. We demonstrate that fat body glycogen, together with the circulating sugar metabolite trehalose, acts as a backup source to maintain glucose availability. The whole-mount PAS staining that we unambiguously evaluated provides an easy and reliable method to assess fat body glycogen in larvae.

We showed that the fat body glycogen is almost completely consumed after 4 h of starvation. Akh derived from the CC has been described to play a crucial role in the mobilization of energy sources, including glycogen, in a broad range of insects (Oudejans et al., 1999; Arrese and Soulages, 2010). Despite the accumulating evidence showing the contribution of CC-derived hormones to glycogen mobilization, we did not observe a significant impact of CC, *Akh* or *AkhR* on the mobilization of fat body glycogen during the larval period. Our results are essentially consistent with those of a recent report using null mutants of *Akh* and *AkhR* (Gáliková et al., 2015). Instead, our results demonstrate that an available glucose level is necessary and sufficient to regulate fat body glycogen in a tissue-autonomous manner. One plausible possibility is that Akh-dependent regulation of carbohydrate metabolism is stage dependent as well as environmental context/species dependent (Gáliková et al., 2015). In agreement with this, the significance of Akh signaling has been reported in *Drosophila* under high-calorie diets or low-yeast diets (Kim and Neufeld, 2015; Song et al., 2017). Because both GlyS and GlyP integrate multiple inputs for the regulation of glycogen metabolism, resulting in changes to the glycemic level, it is reasonable to assume that each developmental period has a distinct regulatory mechanism for energy homeostasis. A responsive tissue-autonomous system has the advantage of rapid adaptation to the depletion of dietary sugar for the maintenance of carbohydrate homeostasis. Consistent with this idea, our results demonstrate that acute deprivation of dietary glucose results in a complete breakdown in fat body glycogen, whereas a diet-dependent adaptation mechanism is initiated to restore fat body glycogen on a long-term basis (Chng et al., 2017). Interestingly, we often observe the mosaic pattern of the PAS signal shortly after starvation and of the uptake levels of 2-NBDG in the fat body. It is likely that the metabolic status, including the glucose uptake ability and starvation response, is not completely identical between individual fat body cells. Together, these observations indicate that carbohydrate metabolism in the fat body is highly adaptable to various dietary conditions during development.

Our results suggest that stored glycogen is degraded under starvation and that the resulting product, glucose phosphate, is likely converted to trehalose in the fat body for circulating sugar homeostasis. We showed that free glucose has much slower decay kinetics than trehalose or glycogen. However, the amount of glucose is much lower than the amount of trehalose in larval hemolymph (Tennessen et al., 2014; Matsuda et al., 2015). Loss of either *Tps1* or *Treh* reduces the circulating glucose levels (Matsuda et al., 2015; Yasugi et al., 2017). Consistently, we observed the continuous activity of Treh both in a fed state and after a brief period of starvation. These results indicate that trehalose metabolism is tightly linked to glucose homeostasis. Therefore, it will be difficult to distinguish whether the fat body produces trehalose or glucose at this stage. Interestingly, the conversion between glycogen and trehalose is not exclusive to starvation. The conversion of glycogen to trehalose has been observed in desiccated larvae of an anhydrobiotic insect (Crowe et al., 1998; Mitsumasu et al., 2010; Cornette and Kikawada, 2011). Similarly, in overwintering insects, stored glycogen is converted to trehalose and sugar alcohols in response to cold stimuli (Rozsypal et al., 2013). These conversions are thought to contribute to the protection of organisms against desiccation and cold injury. By contrast, circulating trehalose can be utilized to synthesize glycogen stored in eggs (Shiomi et al., 1994). Diapause hormone in *Bombyx* stimulates the expression of the trehalase gene in the ovaries, which facilitates the local breakdown of trehalose and the accumulation of glycogen in eggs during the preparative phase of diapause (Su et al., 1994). Therefore, the interconversion between glycogen and trehalose occurs in a tissue-specific manner and is most likely regulated by hormones and various environmental stimuli. The conversion system in any specific organ is likely evolved to provide species-specific physiological tolerance against a wide range of environmental challenges.

In mammals, glycogen is present in the brain, both in astrocytes and in neurons (Duran and Guinovart, 2015). Consistently, we detected glycogen in the larval CNS. We further observed that brain glycogen in larvae is relatively stable under various dietary conditions. On the other hand, it has been reported that the amount of glycogen in the adult fly brain changes between rest and activity (Zimmerman et al., 2004). Interestingly, glycogen in the larval brain is consumed under starvation when circulating trehalose is lacking (Matsuda et al., 2015). These observations suggest that trehalose is the preferred energy source in the larval brain during fasting, whereas internally stored glycogen plays a more important role in adults. Circulating trehalose is hydrolyzed by Treh in surface glia and is further utilized for energy sources in neurons (Volkenhoff et al., 2015; Weiler et al., 2017). Although the insulin/glucagon axis for carbohydrate metabolism is well conserved in *Drosophila*, the regulatory systems of *Drosophila* insulin-like peptide (Dilp) secretion from insulin-producing cells in response to circulating glucose differ significantly between the larval and adult stages (Alfa and Kim, 2016; Nässel and Vanden Broeck, 2016). Therefore, the regulation of trehalose hydrolysis in glia and/or sugar transport activity in the brain might differ between larvae and adults in response to starvation.

In conclusion, our work represents an advance in our understanding of the physiological role of glycogen metabolism. *Drosophila* is a powerful genetic system for studies of the consequence of a tissue-specific metabolic dysregulation at the level of the organism. Because the fat body is one of the central organs for metabolic regulation and glycemic control, our work provides a framework that explains how carbohydrate metabolism is regulated in an organ-dependent manner. It will be of interest to further investigate the environmental context-dependent changes in glycogen metabolism in each organ and glycemic control in different stages of the life cycle.

MATERIALS AND METHODS

Drosophila strains

The following stocks were used: w^{1118} (used as a control), $Tps1^{MI03087}$ (Matsuda et al., 2015), Akh^{A}, Akh^{AP} (Gáliková et al., 2015), $AkhR^{1}$ (Grönke et al., 2007) and $UAS\text{-}Atg1^{K38Q}$ (from T. P. Neufeld, University of Minnesota, Minneapolis, USA). *Tps1-RNAi* lines were obtained from the National Institute of Genetics *Drosophila* RNAi Center. The following stocks were obtained from the Bloomington *Drosophila* Stock Center: $GlyS^{MI01490}$ (34440), *GlyS-RNAi* (34930), *GlyP-RNAi* (33634), *AGBE-RNAi* (40860), *AkhR-RNAi* (29577, 51710), *CG9485/AGL-RNAi* (34333), *InR-RNAi* (35251), *mCherry-RNAi* (35787), *UAS-GFP-Lamp1* (42714), *UAS-p110-CAAX* (25908), *UAS-Akh* (27343) and *Akh-Gal4* (25684). *Tub-Gal4* (5138) and *CG-Gal4* (7011) were used as ubiquitous and fat body-specific Gal4 drivers, respectively. Of note, *CG-Gal4* is also expressed in hemocytes and lymph glands in addition to the fat body during larval development. $GlyS^{MI01490}$ was backcrossed three times with $y^{-}w^{-}$ and used for further analysis on a w^{1118} background.

Development (2018) 145, dev158865. doi:10.1242/dev.158865

Fly food and starvation assay

The animals were reared on fly food that contained 8 g agar, 100 g glucose, 45 g dry yeast, 40 g cornflour, 4 ml propionic acid and 0.45 g butylparaben (in ethanol) per liter (1× recipe). Yeast-only, glucose-only and cornflour-only diets were prepared according to the 1× recipe in H_2O. Maltose and soluble starch were purchased from Wako Pure Chemical Industries and used for the 4% maltose-only or starch-only diet in H_2O. For the analysis of restricted food conditions presented in Fig. 6D, fly food that contained a reduced amount of dry yeast was used (1/5×), as described previously (Matsuda et al., 2015). For the transient starvation experiments, early third-instar larvae (0-3 h after the second ecdysis) were washed in PBS and transferred to a vial that contained 0.8% agar in PBS. All experiments were conducted under noncrowded conditions. No yeast paste was added to the fly tubes for any of the experiments. Quantification of pupal volume was performed as described previously (Okamoto et al., 2013).

qRT-PCR analysis

qRT-PCR analysis was performed as described previously (Okamoto et al., 2012; Okamoto and Nishimura, 2015). The indicated mRNA transcript levels were normalized to the *rp49* (*RpL32* – FlyBase) levels in the same samples. The primers used in this study are listed in Table S1. To directly compare the expression levels of each *GlyS* transcript presented in Fig. S2E, PCR products were cloned into the pCR-BluntII-TOPO vector (Invitrogen) and sequence verified. Serial dilutions of the plasmids were used for the quantification.

Histochemistry

For staining of polysaccharides, including glycogen, larval tissues were dissected in 1% BSA in PBS, fixed using 3.7% formaldehyde in PBS for 20 min, and washed twice with 1% BSA in PBS. Samples were incubated with periodic acid solution (Merck) for 5 min and washed twice with 1% BSA in PBS. Samples were then stained with Schiff's reagent (Merck) for 15 min, washed twice with 1% BSA in PBS, and mounted in 50% glycerol in PBS. For staining of neutral lipids, larval tissues were dissected in PBS, fixed using 3.7% formaldehyde in PBS for 20 min, and washed twice with PBS. Samples were incubated with 0.18% Oil Red O (Sigma-Aldrich) solution in 60% isopropanol for 20 min, washed twice with PBS, and mounted in 50% glycerol in PBS. All procedures described above were carried out at room temperature. Images were acquired with a Zeiss Primo Star microscope equipped with a Zeiss AxioCam ERc. All experiments were independently conducted at least twice and representative images obtained from several larvae are presented.

Immunohistochemistry

Larval tissues were dissected in PBS and fixed for 10 min in 3.7% formaldehyde in PBS containing 0.2% Triton X-100, then processed as previously described (Wirtz-Peitz et al., 2008). Mouse anti-glycogen antibodies (from O. Baba, Tokushima University, Tokushima, Japan), Alexa Fluor dye-conjugated secondary antibodies and phalloidin (Invitrogen) were used. The nuclei were stained with Hoechst 33342 (Invitrogen). Images were acquired with a Zeiss LSM700 confocal microscope and were processed in Photoshop (Adobe Systems).

Ex vivo organ culture experiments

Larval tissues were dissected in PBS and cultured in 1.5 ml tubes at room temperature with rotation. PBS, DMEM (Wako Pure Chemical Industries) or Schneider's medium (Invitrogen) was used as a culture medium, and, when appropriate, glucose (Wako Pure Chemical Industries), 2-deoxyglucose (Wako Pure Chemical Industries) and bovine insulin (Sigma-Aldrich) were added to the medium as indicated. Glucose uptake was analyzed with a fluorescently labeled deoxyglucose, 2-NBDG (Cayman), at 2 mM in PBS for 45 min. The cultured samples were fixed for 10 min in 3.7% formaldehyde in PBS and processed as described above. All experiments were independently conducted at least twice, and representative images obtained from several larvae are presented.

Measurement of protein, TAG and sugar levels

The measurement of protein, TAG, trehalose, glycogen and glucose in whole larvae was performed as described previously (Matsuda et al., 2015).

Measurement of glycogen in each organ

The CNS, fat body and carcass (including the body wall muscles) were dissected from two early third-instar larvae in PBS, transferred to 1.5 ml tubes containing 200 µl cold methanol on ice, and kept at −80°C until extraction. Frozen samples were homogenized in cold methanol with 1×3 µm zirconia beads using a freeze crusher (Tokken). The homogenates were mixed with 100 µl methanol, 50 µl H_2O and 50 µl $CHCl_3$, and incubated at −30°C for 30 min. Samples were centrifuged at 15,000 rpm (20,000 ***g***) for 15 min at 4°C. Glycogen and protein were obtained as insoluble pellet fractions. The pellets were washed with 300 µl ethanol and dried for a few minutes at room temperature. The pellets were then resuspended with 40 µl (the CNS sample) or 160 µl (the fat body and carcass sample) of 0.2× PBS containing 0.1% Triton X-100 and incubated at 70°C for 30 min. Then, 20 µl of each resuspended homogenate was mixed with 10 µl of 0.2× PBS containing amyloglucosidase (Sigma-Aldrich) and incubated overnight at 37°C. The samples were mixed with 400 µl cold methanol, incubated at −30°C for 30 min, and cleared by centrifugation, and the supernatant was vacuum dried. The dried material was resuspended in H_2O, and the absolute amounts of glucose were quantified by liquid chromatography-tandem mass spectrometry (LC-MS/MS) as described below.

The remaining homogenates were mixed with equal volumes of 0.2 N NaOH, heated at 95°C for 15 min and cleared by centrifugation. The supernatants were used for the quantification of protein using a BCA protein assay kit (Thermo Fisher Scientific).

Trehalase activity assay

Trehalase activity assays were performed as described previously (Yoshida et al., 2016). Five early third-instar larvae were used. The amounts of trehalose were quantified by LC-MS/MS.

Quantification of trehalose and glucose by LC-MS/MS

Chromatographic separation and mass spectrometric analysis were performed as described previously (Yoshida et al., 2016; Yasugi et al., 2017).

Statistical analysis

Statistical significance was determined by two-tailed Student's *t*-tests, one-way ANOVA or two-way ANOVA with post hoc test using GraphPad Prism 6 software. Box plots were drawn online using the BoxPlotR application (http://boxplot.tyerslab.com/). Centerlines show the medians, box limits indicate the 25th and 75th percentiles, whiskers extend 1.5 times the interquartile range from the 25th and 75th percentiles, and outliers are represented by dots.

Acknowledgements

We thank O. Baba, T. P. Neufeld, R. Kühnlein, the Bloomington *Drosophila* Stock Center and the National Institute of Genetics *Drosophila* RNAi Center for fly stocks; members of Fly laboratories in RIKEN Center for Developmental Biology for their valuable support and discussion; the Genome Resource and Analysis Unit in RIKEN Center for Life Science Technologies for their support; and S. K. Yoo for critical reading of the manuscript.

Competing interests

The authors declare no competing or financial interests.

Author contributions

Conceptualization: T.Y., T.N.; Methodology: T.Y., T.N.; Validation: O.H., H.K.; Formal analysis: T.Y., T.N.; Investigation: T.Y., O.H., H.K., T.N.; Data curation: T.Y., O.H., H.K., T.N.; Writing - original draft: T.N.; Writing - review & editing: T.Y., T.N.; Visualization: T.Y., T.N.; Supervision: T.N.; Funding acquisition: T.N.

Funding

This work was supported, in part, by the Japan Society for the Promotion of Science (JSPS) [KAKENHI grants JP26711007, JP17K19433 and JP17H03658 to T.N.].

Supplementary information

Supplementary information available online at
http://dev.biologists.org/lookup/doi/10.1242/dev.158865.supplemental

Development (2018) 145, dev158865. doi:10.1242/dev.158865

References

Alfa, R. W. and Kim, S. K. (2016). Using *Drosophila* to discover mechanisms underlying type 2 diabetes. *Dis. Model. Mech.* **9**, 365-376.

Arrese, E. L. and Soulages, J. L. (2010). Insect fat body: energy, metabolism, and regulation. *Annu. Rev. Entomol.* **55**, 207-225.

Baker, K. D. and Thummel, C. S. (2007). Diabetic larvae and obese flies-emerging studies of metabolism in *Drosophila*. *Cell Metab.* **6**, 257-266.

Becker, A., Schlöder, P., Steele, J. E. and Wegener, G. (1996). The regulation of trehalose metabolism in insects. *Experientia* **52**, 433-439.

Bharucha, K. N., Tarr, P. and Zipursky, S. L. (2008). A glucagon-like endocrine pathway in *Drosophila* modulates both lipid and carbohydrate homeostasis. *J. Exp. Biol.* **211**, 3103-3110.

Bouskila, M., Hunter, R. W., Ibrahim, A. F. M., Delattre, L., Peggie, M., van Diepen, J. A., Voshol, P. J., Jensen, J. and Sakamoto, K. (2010). Allosteric regulation of glycogen synthase controls glycogen synthesis in muscle. *Cell Metab.* **12**, 456-466.

Chng, W.-A., Hietakangas, V. and Lemaitre, B. (2017). Physiological adaptations to sugar Intake: new paradigms from *Drosophila melanogaster*. *Trends Endocrinol. Metab.* **28**, 131-142.

Cornette, R. and Kikawada, T. (2011). The induction of anhydrobiosis in the sleeping chironomid: current status of our knowledge. *IUBMB Life* **63**, 419-429.

Crowe, J. H., Carpenter, J. F. and Crowe, L. M. (1998). The role of vitrification in anhydrobiosis. *Annu. Rev. Physiol.* **60**, 73-103.

Droujinine, I. A. and Perrimon, N. (2016). Interorgan communication pathways in physiology: focus on *Drosophila*. *Annu. Rev. Genet.* **50**, 539-570.

Duran, J. and Guinovart, J. J. (2015). Brain glycogen in health and disease. *Mol. Aspects Med.* **46**, 70-77.

Duran, J., Tevy, M. F., Garcia-Rocha, M., Calbó, J., Milán, M. and Guinovart, J. J. (2012). Deleterious effects of neuronal accumulation of glycogen in flies and mice. *EMBO Mol. Med.* **4**, 719-729.

Eanes, W. F., Merritt, T. J. S., Flowers, J. M., Kumagai, S., Sezgin, E. and Zhu, C.-T. (2006). Flux control and excess capacity in the enzymes of glycolysis and their relationship to flight metabolism in *Drosophila melanogaster*. *Proc. Natl. Acad. Sci. USA* **103**, 19413-19418.

Elbein, A. D., Pan, Y. T., Pastuszak, I. and Carroll, D. (2003). New insights on trehalose: a multifunctional molecule. *Glycobiology* **13**, 17R-27R.

Gáliková, M., Diesner, M., Klepsatel, P., Hehlert, P., Xu, Y., Bickmeyer, I., Predel, R. and Kühnlein, R. P. (2015). Energy homeostasis control in *Drosophila* adipokinetic hormone mutants. *Genetics* **201**, 665-683.

Garrido, D., Rubin, T., Poidevin, M., Maroni, B., Le Rouzic, A., Parvy, J.-P. and Montagne, J. (2015). Fatty acid synthase cooperates with glyoxalase 1 to protect against sugar toxicity. *PLoS Genet.* **11**, e1004995.

Grönke, S., Müller, G., Hirsch, J., Fellert, S., Andreou, A., Haase, T., Jäckle, H. and Kühnlein, R. P. (2007). Dual lipolytic control of body fat storage and mobilization in *Drosophila*. *PLoS Biol.* **5**, e137.

Gutierrez, E., Wiggins, D., Fielding, B. and Gould, A. P. (2007). Specialized hepatocyte-like cells regulate Drosophila lipid metabolism. *Nature* **445**, 275-280.

Kim, J. and Neufeld, T. P. (2015). Dietary sugar promotes systemic TOR activation in *Drosophila* through AKH-dependent selective secretion of Dilp3. *Nat. Commun.* **6**, 6846.

Kim, S. K. and Rulifson, E. J. (2004). Conserved mechanisms of glucose sensing and regulation by *Drosophila* corpora cardiaca cells. *Nature* **431**, 316-320.

Lee, G. and Park, J. H. (2004). Hemolymph sugar homeostasis and starvation-induced hyperactivity affected by genetic manipulations of the adipokinetic hormone-encoding gene in *Drosophila melanogaster*. *Genetics* **167**, 311-323.

Leopold, P. and Perrimon, N. (2007). *Drosophila* and the genetics of the internal milieu. *Nature* **450**, 186-188.

Matsuda, H., Yamada, T., Yoshida, M. and Nishimura, T. (2015). Flies without trehalose. *J. Biol. Chem.* **290**, 1244-1255.

Mitsumasu, K., Kanamori, Y., Fujita, M., Iwata, K.-I., Tanaka, D., Kikuta, S., Watanabe, M., Cornette, R., Okuda, T. and Kikawada, T. (2010). Enzymatic control of anhydrobiosis-related accumulation of trehalose in the sleeping chironomid, *Polypedilum vanderplanki*. *FEBS J.* **277**, 4215-4228.

Nässel, D. R. and Vanden Broeck, J. (2016). Insulin/IGF signaling in *Drosophila* and other insects: factors that regulate production, release and post-release action of the insulin-like peptides. *Cell Mol. Life Sci.* **73**, 271-290.

Okamoto, N. and Nishimura, T. (2015). Signaling from glia and cholinergic neurons controls nutrient-dependent production of an insulin-like peptide for *Drosophila* body growth. *Dev. Cell* **35**, 295-310.

Okamoto, N., Nishimori, Y. and Nishimura, T. (2012). Conserved role for the Dachshund protein with *Drosophila* Pax6 homolog Eyeless in insulin expression. *Proc. Natl. Acad. Sci. USA* **109**, 2406-2411.

Okamoto, N., Nakamori, R., Murai, T., Yamauchi, Y., Masuda, A. and Nishimura, T. (2013). A secreted decoy of InR antagonizes insulin/IGF signaling to restrict body growth in *Drosophila*. *Genes Dev.* **27**, 87-97.

Oudejans, R. C. H. M., Harthoorn, L. F., Diederen, J. H. B. and van der Horst, D. J. (1999). Adipokinetic hormones: coupling between biosynthesis and release. *Ann. NY Acad. Sci.* **897**, 291-299.

Parvy, J.-P., Napal, L., Rubin, T., Poidevin, M., Perrin, L., Wicker-Thomas, C. and Montagne, J. (2012). *Drosophila melanogaster* Acetyl-CoA-carboxylase sustains a fatty acid-dependent remote signal to waterproof the respiratory system. *PLoS Genet.* **8**, e1002925.

Petersen, M. C., Vatner, D. F. and Shulman, G. I. (2017). Regulation of hepatic glucose metabolism in health and disease. *Nat. Rev. Endocrinol.* **13**, 572-587.

Roach, P. J., Depaoli-Roach, A. A., Hurley, T. D. and Tagliabracci, V. S. (2012). Glycogen and its metabolism: some new developments and old themes. *Biochem. J.* **441**, 763-787.

Rozsypal, J., Koštál, V., Zahradníčková, H. and Šimek, P. (2013). Overwintering strategy and mechanisms of cold tolerance in the codling moth (*Cydia pomonella*). *PLoS ONE* **8**, e61745.

Ruaud, A.-F., Lam, G. and Thummel, C. S. (2011). The *Drosophila* NR4A nuclear receptor DHR38 regulates carbohydrate metabolism and glycogen storage. *Mol. Endocrinol.* **25**, 83-91.

Saez, I., Duran, J., Sinadinos, C., Beltran, A., Yanes, O., Tevy, M. F., Martínez-Pons, C., Milán, M. and Guinovart, J. J. (2014). Neurons have an active glycogen metabolism that contributes to tolerance to hypoxia. *J. Cereb. Blood Flow Metab.* **34**, 945-955.

Saltiel, A. R. and Kahn, C. R. (2001). Insulin signalling and the regulation of glucose and lipid metabolism. *Nature* **414**, 799-806.

Scott, R. C., Schuldiner, O. and Neufeld, T. P. (2004). Role and regulation of starvation-induced autophagy in the *Drosophila* fat body. *Dev. Cell* **7**, 167-178.

Shiomi, K., Ishida, Y., Ikeda, M., Sato, Y., Saito, H., Imai, K., Isobe, M. and Yamashita, O. (1994). Induction of non-diapause eggs by injection of anti-diapause hormone rabbit serum into the diapause type of the silkworm, *Bombyx mori*. *J. Insect Physiol.* **40**, 693-699.

Shukla, E., Thorat, L. J., Nath, B. B. and Gaikwad, S. M. (2015). Insect trehalase: physiological significance and potential applications. *Glycobiology* **25**, 357-367.

Sinadinos, C., Valles-Ortega, J., Boulan, L., Solsona, E., Tevy, M. F., Marquez, M., Duran, J., Lopez-Iglesias, C., Calbó, J., Blasco, E. et al. (2014). Neuronal glycogen synthesis contributes to physiological aging. *Aging Cell* **13**, 935-945.

Song, W., Cheng, D., Hong, S., Sappe, B., Hu, Y., Wei, N., Zhu, C., O'Connor, M. B., Pissios, P. and Perrimon, N. (2017). Midgut-derived activin regulates glucagon-like action in the fat body and glycemic control. *Cell Metab.* **25**, 386-399.

Su, Z.-H., Ikeda, M., Sato, Y., Saito, H., Imai, K., Isobe, M. and Yamashita, O. (1994). Molecular characterization of ovary trehalase of the silkworm, *Bombyx mori* and its transcriptional activation by diapause hormone. *Biochim. Biophys. Acta* **1218**, 366-374.

Teleman, A. A. (2009). Molecular mechanisms of metabolic regulation by insulin in *Drosophila*. *Biochem. J.* **425**, 13-26.

Tennessen, J. M., Barry, W. E., Cox, J. and Thummel, C. S. (2014). Methods for studying metabolism in *Drosophila*. *Methods* **68**, 105-115.

Unger, R. H. (1971). Glucagon and the insulin: glucagon ratio in diabetes and other catabolic illnesses. *Diabetes* **20**, 834-838.

Volkenhoff, A., Weiler, A., Letzel, M., Stehling, M., Klämbt, C. and Schirmeier, S. (2015). Glial glycolysis is essential for neuronal survival in *Drosophila*. *Cell Metab.* **22**, 437-447.

Weiler, A., Volkenhoff, A., Hertenstein, H. and Schirmeier, S. (2017). Metabolite transport across the mammalian and insect brain diffusion barriers. *Neurobiol. Dis.* **107**, 15-31.

Wigglesworth, V. B. (1949). The utilization of reserve substances in *Drosophila* during flight. *J. Exp. Biol.* **26**, 150-163.

Wirtz-Peitz, F., Nishimura, T. and Knoblich, J. A. (2008). Linking cell cycle to asymmetric division: aurora-A phosphorylates the Par complex to regulate Numb localization. *Cell* **135**, 161-173.

Yasugi, T., Yamada, T. and Nishimura, T. (2017). Adaptation to dietary conditions by trehalose metabolism in *Drosophila*. *Sci. Rep.* **7**, 1619.

Yoshida, M., Matsuda, H., Kubo, H. and Nishimura, T. (2016). Molecular characterization of Tps1 and Treh genes in *Drosophila* and their role in body water homeostasis. *Sci. Rep.* **6**, 30582.

Zimmerman, J. E., Mackiewicz, M., Galante, R. J., Zhang, L., Cater, J., Zoh, C., Rizzo, W. and Pack, A. I. (2004). Glycogen in the brain of *Drosophila melanogaster*: diurnal rhythm and the effect of rest deprivation. *J. Neurochem.* **88**, 32-40.

Zirin, J., Nieuwenhuis, J. and Perrimon, N. (2013). Role of autophagy in glycogen breakdown and its relevance to chloroquine myopathy. *PLoS Biol.* **11**, e1001708.

Zirin, J., Nieuwenhuis, J., Samsonova, A., Tao, R. and Perrimon, N. (2015). Regulators of autophagosome formation in *Drosophila* muscles. *PLoS Genet.* **11**, e1005006.

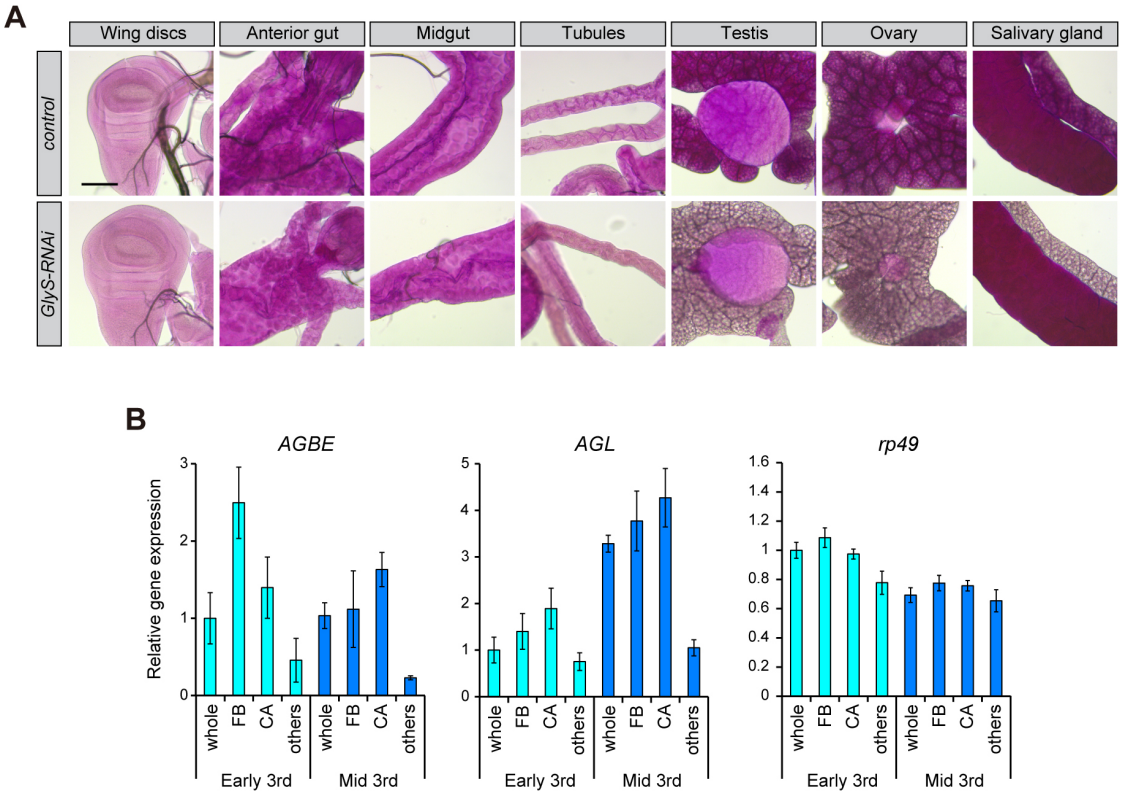

Figure S1. Tissue distribution and visualization of glycogen in larvae.

(A) PAS staining does not reliably detect stored glycogen in the imaginal discs, midgut, Malpighian tubules, testes, ovaries, or salivary glands under our experimental conditions. Stored glycogen was judged by the difference between control and *GlyS*-knockdown larvae. *Tub-Gal4* was used for ubiquitous knockdown. Of note, the results of PAS staining do not rule out the presence of glycogen in each tissue. Scale bars: 100 μm. (B) The tissue distributions of the gene transcripts related to glycogen metabolism were analyzed by qRT-PCR in early third-instar and mid third-instar larvae. whole, whole larva; FB, fat body; CA, carcass including body wall muscles; others, midgut and CNS. Relative changes in the *rp49* levels across tissues are also shown. The values shown are means and SD ($n = 4$).

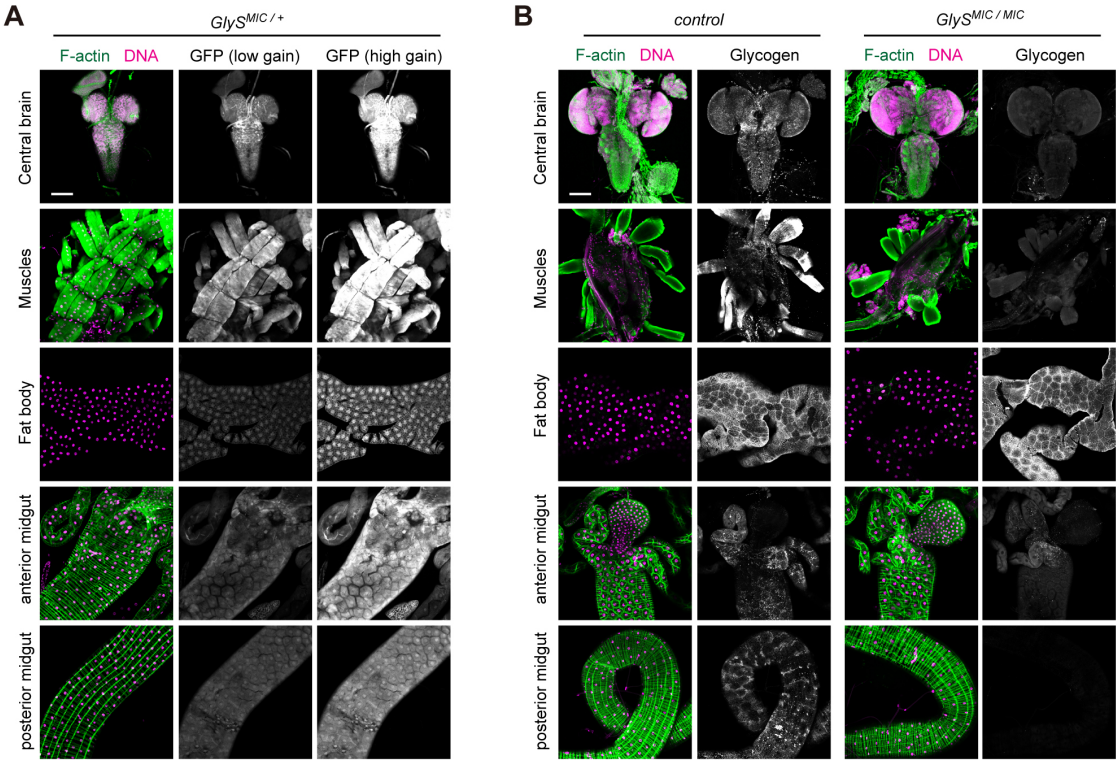

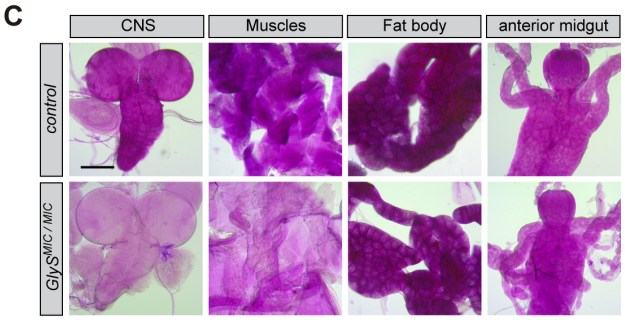

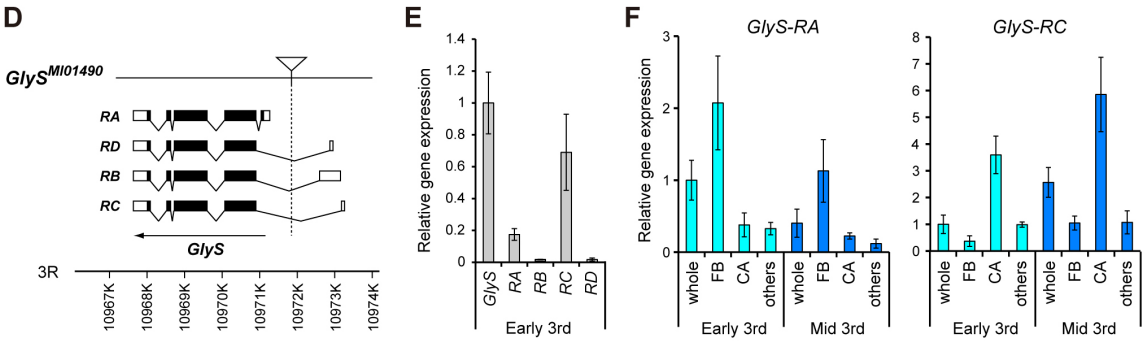

Figure S2. Characterization of a line with a *Minos* insertion in the *GlyS* gene locus. (A) GFP reporter expression of $GlyS^{MI01490}$ (named $GlyS^{MIC}$) was analyzed in each tissue. GFP expression is mainly detected in the muscles and CNS, and weak expression of GFP is detectable in the fat body and midgut. Two different imaging conditions are shown. (B) $GlyS^{MIC}$ homozygous mutants have significantly reduced amounts of glycogen in the brain, muscles, and midgut, but not in the fat body. Glycogen was visualized by immunostaining with anti-glycogen antibody. (C) Glycogen was visualized in each tissue by PAS staining. $GlyS^{MIC}$ homozygous mutants had significantly reduced brain glycogen and muscle glycogen, but the fat body glycogen was unaffected. Notably, glycogen stored in the midgut was accurately detected by immunostaining with anti-glycogen antibody, but not by PAS staining under these conditions. (D) Schematic representation of the *GlyS* locus. Protein-coding regions and untranslated regions are represented by black boxes and white boxes, respectively. The *Minos* insertion site, $GlyS^{MI01490}$, is marked with an inverted triangle. (E) Expression of *GlyS* transcripts in early third-instar larvae was analyzed by qRT-PCR. Serial dilutions of plasmids carrying cDNAs were used for standards. The relative expression levels are shown after the absolute quantification of mRNAs. (F) Tissue-dependent expression of *GlyS* transcripts was analyzed by qRT-PCR. The *GlyS-RA* transcript is mainly expressed in the fat body, whereas the *GlyS-RC* transcript is mainly expressed in the carcass, including the body wall muscles. whole, whole larva; FB, fat body; CA, carcass including body wall muscles; others, midgut and CNS. The values shown are means and SD. n = 4 [E, F]. Scale bars: 100 μm.

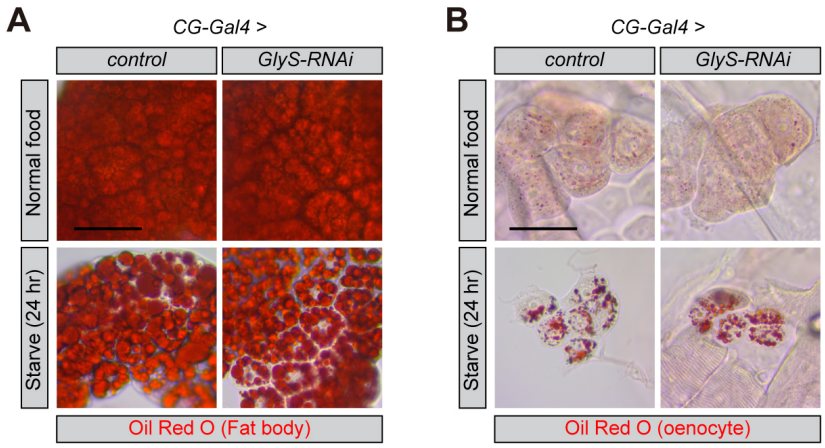

Figure S3. Loss of fat body glycogen does not significantly affect the mobilization of triglycerides.

(A) Knockdown of *GlyS* in the fat body does not affect the mobilization of lipid droplets in the fat body under starvation. (B) Knockdown of *GlyS* in the fat body does not affect the accumulation of lipid droplets in oenocytes upon starvation. Lipid droplets were visualized by Oil Red O staianing. Early third-instar larvae of the indicated genotypes were cultured on a normal food or agar-only diet for 24 hours. Scale bars: 50 μm.

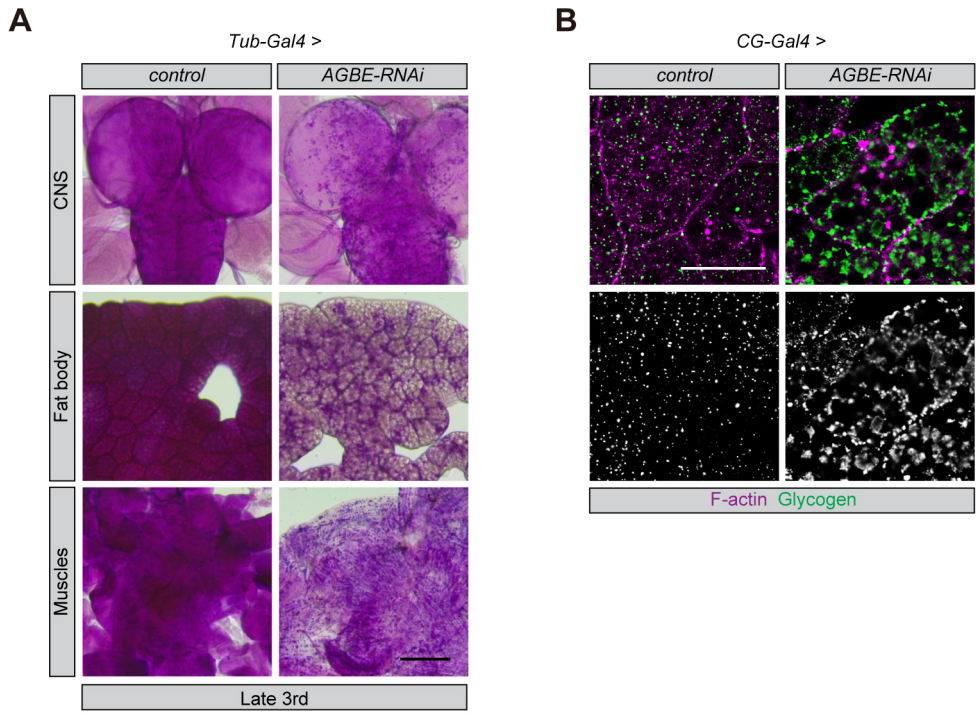

Figure S4. Knockdown of *AGBE* causes the aggregation of glycogen.

(A) Knockdown of *AGBE* causes the aggregation of glycogen. *Tub-Gal4* was used for ubiquitous knockdown. Glycogen in each tissue was visualized by PAS staining in late third-instar larvae. Scale bars: 100 μm. (B) Fat body glycogen was visualized by immunostaining with anti-glycogen antibody. Scale bars: 50 μm.

Figure S5. Sequence comparison of *Drosophila* GlyS and GlyP to mammalian GYS2 and PYGL.

(A) Amino acid sequence alignment of *Drosophila* GlyS and human liver glycogen synthase (GYS2). (B) Amino acid sequence alignment of *Drosophila* GlyP and human liver glycogen phosphorylase (PYGL). Identical and similar residues between the sequences are indicated by asterisks and colons, respectively. Blue colors indicate the amino acid sequence, which is unique in the *GlyS-RA* isoform. Red colors indicate the conserved phosphorylation sites, which regulate the enzyme activities. The amino acid sequence alignments were made using the ClustalW program. Human GYS2 RefSeq: NP_068776.2; Human PYGL RefSeq: NP_002854.3.

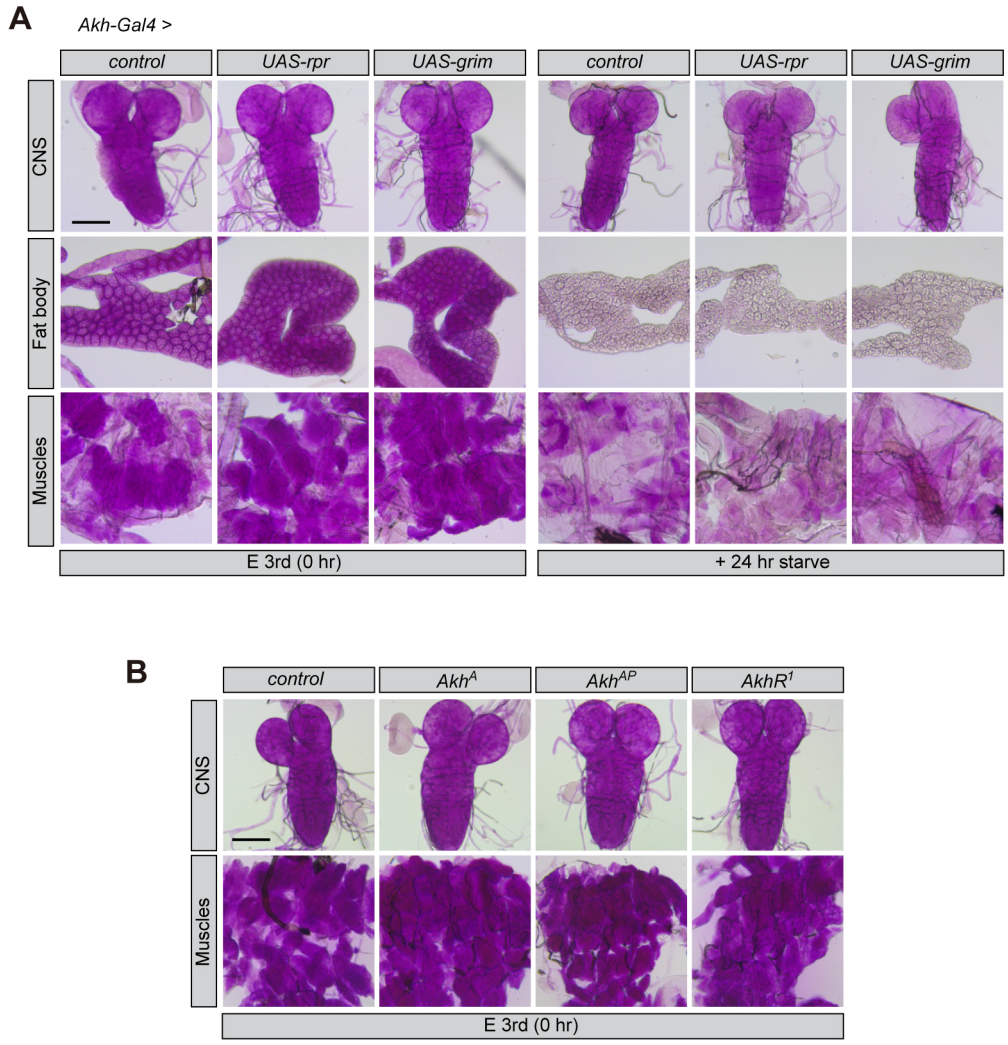

Figure S6. Akh signaling does not affect the steady-state levels or mobilization of muscle glycogen and brain glycogen in larvae.

(A) Loss of Akh-producing cells has no significant impact on the steady-state levels or mobilization of glycogen in muscles and the central nervous system (CNS). Glycogen was analyzed by PAS staining at the indicated time points. Early third-instar larvae (E 3rd) were used for the experiments. (B) The Akh^{A}, Akh^{AP}, and $AkhR^{1}$ mutants display no abnormalities at the steady-state levels of glycogen in muscles and the CNS. Scale bars: 100 μm.

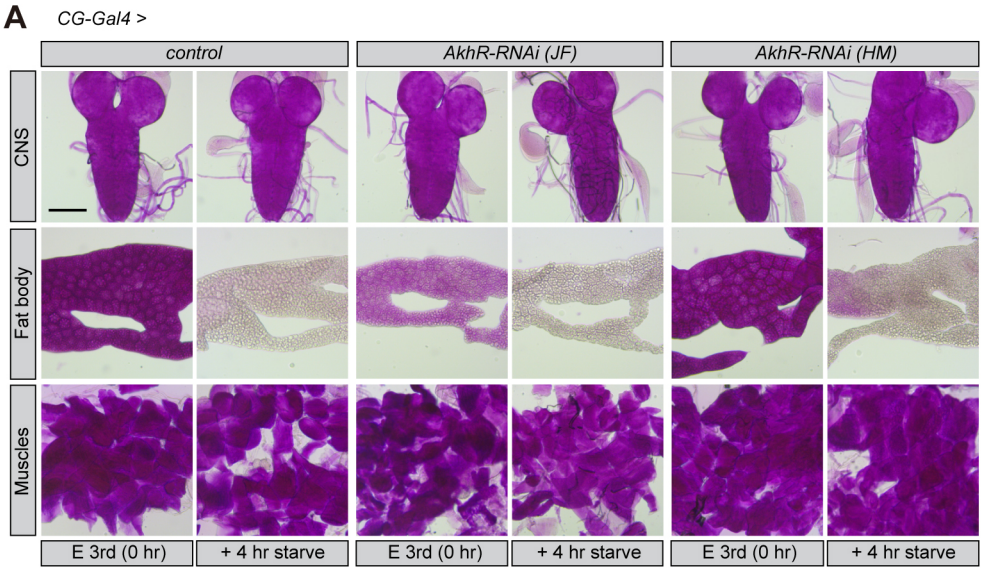

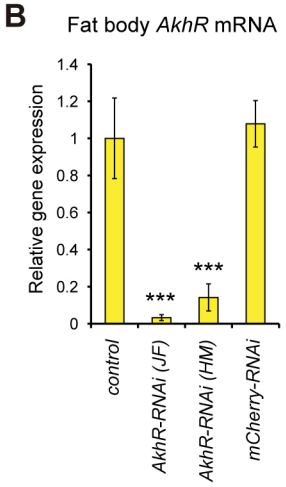

C

		Phenotype	Pupariation
CG-Gal4	*AkhR-RNAi (JF)*	viable	1 day delay
	AkhR-RNAi (HM)	viable	no delay
tub-Gal4	*AkhR-RNAi (JF)*	late pupal lethal	1∼2 days delay
	AkhR-RNAi (HM)	viable	no delay
Akh-Gal4	*UAS-rpr*	viable	no delay
	UAS-grim	viable	no delay

	Lethality	Pupariation
Akh^{A}	viable	no delay
Akh^{AP}	viable	no delay
$AkhR^{1}$	viable	no delay

Figure S7. Knockdown of *AkhR* in the fat body does not affect the mobilization of fat body glycogen.

(A) Steady-state levels and the mobilization of fat body glycogen were analyzed after knockdown of *AkhR* in the fat body. Although *AkhR-RNAi* (JF; BDSC#29577), but not *AkhR-RNAi* (HM; BDSC#51710), showed a decrease in the steady-state levels of fat body glycogen, mobilization after starvation occurred normally in both cases. Glycogen was analyzed by PAS staining at the indicated time points. Early third-instar larvae (E 3rd) were used for the experiments. Scale bars: 100 μm. (B) Knockdown of *AkhR* was confirmed by qRT-PCR in the dissected fat body from early third-instar larvae. The values shown are means and SD ($n = 4$). ***P<0.001; one-way ANOVA with Dunnett's post hoc test. (C) Summary of the *Akh* and *AkhR* mutants and *AkhR* knockdown

phenotype. Consistent with previous reports (Grönke et al., 2007; Gáliková et al., 2015), the Akh^{A}, Akh^{AP}, and $AkhR^{1}$ mutants display no lethality and no developmental delays under the standard diet conditions used in this study. Consistently, genetic ablation of the Akh-producing cells resulted in no lethality. It should be noted, however, that *AkhR-RNAi* (JF) displayed a growth defect and developmental delay when crossed with *CG-Gal4* and caused late pupal lethality (100% penetrance) when crossed with *tub-Gal4* under these conditions. *AkhR-RNAi* (HM) did not display such lethality upon ubiquitous expression. Therefore, *AkhR-RNAi* (JF) has off-target effect(s).

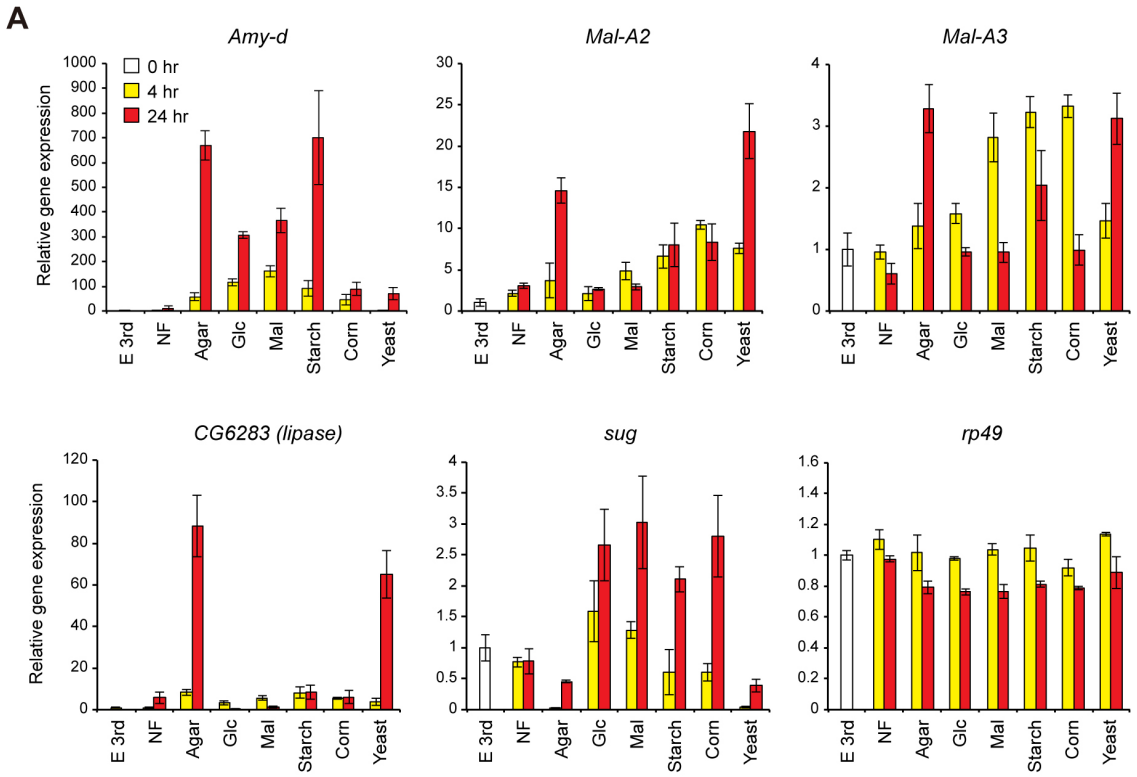

Figure S8. Changes in the expression level of digestive enzymes in larvae.

(A) The expression levels of digestive enzymes were analyzed by qRT-PCR under various dietary conditions. The feeding of a maltose-only (Mal), starch-only (Starch) or cornflour-only (Corn) diet induced the expression of maltase, namely, *Mal-A2* and *Mal-A3*, whereas the feeding of a glucose-only (Glc) did not. Continuous feeding of a maltose-only, starch-only or cornflour-only diet suppressed the further induction of *Mal-A2* and *Mal-A3*, whereas the continuous feeding of an agar-only (Agar) or a yeast-only (Yeast) diet up-regulated *Mal-A2* and *Mal-A3* in a time-dependent manner. The induction of an amylase, *Amy-d,* under starvation was in part suppressed by a glucose-only or maltose-only diet and strongly suppressed by a cornflour-only or yeast-only diet. Under these conditions, a sugar-responsive transcription factor, *sugerbabe* (*sug*), was up-regulated under carbohydrate-rich dietary conditions, while a digestive lipase, named *CG6283*, was induced under carbohydrate-poor dietary conditions. Of note, *Amy-d*, *Mal-A2*, *Mal-A3*, and *CG6283* are predominantly expressed in the midgut (Flybase). NF, normal food. The values shown are means and SD (n = 3). The relative changes in the *rp49* levels between conditions are also shown.

rp49 sense	CAGTCGGATCGATATGCTAAGCTG
rp49 antisense	TAACCGATGTTGGGCATCAGATAC
Tps1 sense	TCCGATGAGATCCTACAGGGTATG
Tps1 antisense	CGCCATGTTCCACCAGCAGATTG
Tret1-1 sense	ATGTCTCCGACATCGCCATGGTTC
Tret1-1 antisense	TCACCCATCATCAGCCAGGGAATG
GlyS sense	TTGCGCGATACGATCAACAACGTC
GlyS antisense	CGGATCATTCCAGTCATCAGCCAC
GlyP sense	CAACTGGTTGCTCTGAAGAAGTGG
GlyP antisense	CTGGCGCTTGTACTCGTGAATACG
AGBE sense	GCGAGGCGTACCTGAACTTTATGG
AGBE antisense	TCATTCATGGCTCGATCGAATTCG
CG9485/AGL sense	GCTTGACCATGCAGAGTGACAAGC
CG9485/AGL antisense	CGTAGATTGGCAAAGTTTAGCTCC
GlyS-RA sense	GATGCGCAGACAGCAGTCCTACCG
GlyS-RB sense	GTGAGATAGCACTTCATTTTCACC
GlyS-RC sense	TGTTTCGTGTGGCCAACAACAGCG
GlyS-RD sense	ACGGCAACAACAATTGATGAATCG
GlyS-RA/B/C/D common antisense	ACCGGATCACCGTGTAAATACCGC
Amy-d sense	TCAGAGTGAAATTTAGCTTCCACC
Amy-p sense	GAGTGAAACTGAACTTCCATCTGG
Amy-d/p common antisense	CCTTGACGGCGTTCTCGTTCACAG
Mal-A2 sense	TTCTAATTTCCACCACCCAGGAGG
Mal-A2 antisense	CATAAAAGTTAGAGATGTCGTAGC
Mal-A3 sense	TCAGTTCTACCAGATCTATCCCAG
Mal-A3 antisense	GGGCCTCGAAATCCTCCATTGTGC
Mal-A4 sense	ATGACCACTTGGACTAGCTTGTTC
Mal-A4 antisense	TGTCATAGCCAAAGTCTGCCATCG
CG6283 sense	TGCCGCCTTACTGGCAGCCGTGAG
CG6283 antisense	GAGCCGGACTTGGCCTTGATCTCC

Table S1.

Primers used for qRT-PCR analyses.